MLM-1642

THE EFFECTIVE ALPHA ACTIVITY OF PLUTONIUM-238 DIOXIDE MICROSPHERES

G. N. Huffman

AEC Research and Development REPORT

MONSANTO RESEARCH CORPORATION

A SUBSIDIARY OF MONSANTO COMPANY

MOUND LABORATORY

MIAMISBURG, OHIO

OPERATED FOR

UNITED STATES ATOMIC ENERGY COMMISSION

U.S. GOVERNMENT CONTRACT NO. AT-33-1-GEN-53

DISCLAIMER

Printed in the United States of America
Available from
Clearinghouse for Federal Scientific and Technical Information
National Bureau of Standards, U. S. Department of Commerce
Springfield, Virginia 22151
Price: Printed Copy $3.00; Microfiche $0.65

LEGAL NOTICE

MLM-1642
TID-4500
UC-4 Chemistry

THE EFFECTIVE ALPHA ACTIVITY OF PLUTONIUM-238 DIOXIDE MICROSPHERES

G. N. Huffman

Issued: April 1969

MONSANTO RESEARCH CORPORATION

A SUBSIDIARY OF MONSANTO COMPANY

MOUND LABORATORY

MIAMISBURG, OHIO

OPERATED FOR

UNITED STATES ATOMIC ENERGY COMMISSION

U.S. GOVERNMENT CONTRACT NO. AT-33-1-GEN-53

THE EFFECTIVE ALPHA ACTIVITY OF PLUTONIUM-238 DIOXIDE MICROSPHERES

Thesis

Submitted to

The College of Arts and Sciences

University of Dayton

In Partial Fulfillment of the Requirements for

The Degree

Master of Science in Chemistry

by

Gary N. Huffman

College of Arts and Sciences

University of Dayton

Dayton, Ohio

April, 1969

APPROVED BY:

(Faculty Advisor)

(Faculty Reader)

(Faculty Reader)

(Industrial Advisor)

ACKNOWLEDGEMENT

I wish to thank everyone who contributed in some way to the progress of this study. Special thanks go to Dr. Carl Kershner for the many hours spent deriving mathematical relationships and Allen Campbell for his complete cooperation and valuable advice.

My wife and three sons should not be forgotten, because without their help, encouragement, and understanding, this study would never have been started.

CONTENTS

LIST OF TABLES

LIST OF ILLUSTRATIONS

LIST OF TABLES IN APPENDIX A

LIST OF EXAMPLE CALCULATIONS IN APPENDIX B

INTRODUCTION

I. Purpose

The purpose of this study was to determine the effective alpha activity of plutonium-238 dioxide microspheres as a function of their spherical diameters. The effective alpha activity is here defined as that portion of the total alpha particles emitted by the plutonium atoms that escape from the surface of the microsphere. Because of recently developed theories relating the effective alpha activity of microspheres to the range of an alpha particle in the medium of these microspheres, a second purpose of this study was to determine the range of an alpha particle in plutonium-238 dioxide using these theories, and thus obtain evidence to verify the theories. This study is important because effective activity values are needed for radiolysis calculations in the fields of radiation chemistry and radiological health.

II. Background

"Swift Particles", i.e., particles whose velocities are much higher than the velocities of thermal agitation, are generally divided into two groups. The first group is "light particles" whose masses are on the order of an electron's. The second group is "heavy particles" which are defined as including all particles whose rest mass is large compared with that of an electron.[1] Obviously, alpha particles, which are helium nuclei, fall into the second group.

The range in a medium is generally defined as the projection of the path length in the medium on the path direction prior to incidence with the medium.[2] While light particles are easily deflected, heavy particles are too massive to be strongly deflected and their path length is so nearly equal to its projection on the incident path that they are said to have a "definite" range.[3] The interactions which effect the range of swift particles are primarily coulombic in nature. This includes ionization, scattering, and various types of radiative losses. These interactions may be classified into four basic types:[1] inelastic and elastic collision with an absorber electron, and inelastic and

elastic collision with an absorber nucleus. Of these four basic types, the most probable interaction for the 5.5 Mev alpha particle emitted by plutonium-238 is inelastic collision with an absorber electron and this is the predominate method by which alpha particles loose their kinetic energy. When an alpha particle inelastically collides with an electron, it experiences transition to an excited state (excitation) or to an unbound state (ionization). An alpha particle looses approximately 35 ev per ion pair formed.

There are numerous theories for describing these individual encounters. However, the range of an alpha particle is the result of the statistical average of all the pertinent interactions. As such, range-energy relationships for swift particles are almost purely empirical.[1]

As early as 1904, W. H. Bragg measured the range of alpha particles in air using an ionization chamber.[4] In analyzing the results of his study, he concluded that the "stopping power",[5] i.e., the rate of loss of energy with respect to distance $-\left(\frac{dE}{dx}\right)$, is nearly constant over that portion of the range in which the alpha particle still possesses kinetic energy greater than 1 Mev.

An empirical rule, called Bragg's rule,[6] is one result of treating the stopping power as a constant. Bragg's rule states that the atomic stopping power of an absorber (i.e., the stopping effect per atom) is about proportional to the square root of the atomic weight.

A useful consequence of Bragg's rule is the Bragg-Kleeman Rule.[7] Mathematically, it is expressed:

$$\frac{R_1}{R_0} = \frac{\rho_0 \sqrt{A_1}}{\rho_1 \sqrt{A_0}}$$

Where R_0 and R_1 are the ranges of alpha particles of equal energy in different mediums, ρ_0 and ρ_1 are the respective densities of those mediums, and A_0 and A_1 are the atomic weights for the elements of which the mediums are composed. The quantities $\sqrt{A_0}$ and $\sqrt{A_1}$ are called the effective atomic weights of the mediums. For substances composed of more than one element, the effective atomic weight is:

$$\sqrt{A} = \frac{n_1 \quad A_1 + n_2 \quad A_2 + n_3 \quad A_3 + \ldots}{n_1 \sqrt{A_1} + n_2 \sqrt{A_2} + n_3 \sqrt{A_3} + \ldots}$$

where n_1, n_2, etc. are the atomic fractions for the elements in the compound and A_1, A_2, etc. are the atomic weights for

the elements in the compound. For air, which is commonly used in such calculations, $\sqrt{A_0} = 3.82\ (gm)^{\frac{1}{2}}$ and $\rho_0 = 1.226 \times 10^{-3}$ (gm/cm^3) at 15°C and 760 mm Hg. The Bragg-Kleeman rule now reduces to,

$$R_1 = 3.2 \times 10^{-4} \frac{\sqrt{A_1}}{\rho_1} R_{air}$$

Ranges are reported in one of two ways.[4] First, as the distance traveled in a medium in some convenient units, e.g., centimeters or microns. Second, as the areal density, thickness-density, density-thickness, or equivalent thickness. All of these terms mean the same thing mathematically:

$$\text{Equivalent thickness } (mg/cm^2) = \text{Actual thickness } (cm) \times \text{density } (gm/cm^3) \div 1000$$

Throughout this paper, ranges will be reported as the distance traveled in microns.

It should be understood that the ranges of alpha particles emitted at a homogeneous energy assume a narrow distribution. This is due to an effect called "straggling".[4],[5] As an alpha particle slows due to loss of energy by the formation of ion pairs, it begins to spend more time in the neighborhood of

each absorber atom. At first, the number of ion pairs formed per unit distance increases sharply. However, at about 370 Kev the alpha particle has slowed to the point where the probability that at first one, and then two electrons will adhere to it, also increases sharply. The He^+ ion thus formed has less ionizing power than an alpha particle (i.e., an He^{2+} ion) and the He° atom has no ionizing power. Since the range of an alpha particle is detected by its ability to form ion pairs, when a helium atom is formed, this is the end of the range. However, it is possible for either the He° atom or He^+ ion to give up its electron in a subsequent collision and regain its ionizing power at which point it can be detected again. This sequence of events termed straggling results in a distribution of ranges, the average of which is called the mean range ($\bar{R}$). It is the mean range that is measured in this study.

Theory

C. J. Kershner[8] first proposed the theory that the range of an alpha particle in PuO_2 microspheres could be determined by measuring their diameters and the ratio of the effective activity to the total activity. His relationship can be derived by considering that dn_i is the number of particles escaping per second from a region of volume dv_i below the surface of the microspheres where n_o is the total disintegrations per second per cubic centimeter and A_ρ/A_γ is the ratio of the area of the spherical zone (see Fig. 1) and the total sphere of emission of radius R (where R is the range of an alpha particle). Then,

$$\frac{dn_i}{n_o} = \frac{A_\rho}{A} \, dv_i \qquad [1]$$

substituting $A_\rho = 2\pi R h_i$ and $A_\gamma = 4\pi R^2$, equation [1] becomes:

$$dn_i = \frac{n_o h_i}{2R} \, dv_i \qquad [2]$$

Before this equation can be integrated, you must substitute for h_i.

$$y^2 + (\rho + R - h_i)^2 = r^2 \qquad [3]$$

$$y^2 + (R - h_i)^2 = R^2 \qquad [4]$$

Mathematical Model for Kershner's Effective Activity Theory

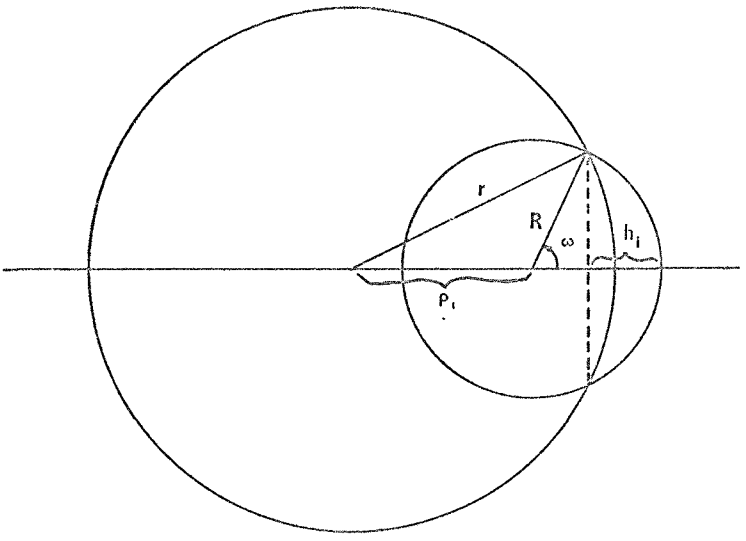

Integration of this equation

$$\int_0^n dn = \frac{8No}{2R} \int_0^{\pi/2} \int_0^{\pi/2} \int_{|\vec{r}-R|}^{r} \left(R + \rho/2 - \frac{r^2-R^2}{2\rho}\right) \rho^2 \, d\rho \, \sin\varphi \, d\varphi \, d\theta$$

arrived at through geometrical considerations in the above diagram yields the effective activity

$$n = 4/3 \, \pi r^3 n_o \left[\frac{R}{16r} - \left(12 - \frac{R^2}{r^2}\right)\right]$$

Since the total alpha emission from the plutonium in the microsphere is $4/3 \, \pi r^3 n_o$,

$$f = \frac{R}{16r}\left(12 - \frac{R^2}{r^2}\right)$$

FIGURE 1

Eliminating y^2 and solving for h_i you obtain equation [5]

$$h_i = R + \rho_i/2 - \frac{r^2 - R^2}{2\rho_i} \qquad [5]$$

Therefore,

$$dn_i = \frac{n_o}{2R}\left(R + \rho_i/2 - \frac{r^2 - R^2}{2\rho_i}\right) dv_i \qquad [6]$$

By substituting the spherical coordinate volume integral for dv_i, the integral form of equation [6] becomes:

$$\int_o^n dn = \frac{8n_o}{2R}\int_{|R-r|}^{r}\int_o^{\pi/2}\int_o^{\pi/2}\left(R + \rho/2 - \frac{r^2 - R^2}{2\rho}\right)\rho^2 \sin\varphi d\varphi d\theta d\rho \qquad [7]$$

Notice that a multiplication factor of eight is required since the integration limits of θ and φ sum only over the first octant of the source sphere.

The integration limits on ρ result from the fact that it can be shown that if $R \leq r$, you must integrate from $(r - R)$ to r, but if $2r \leq R \leq r$, you must integrate from $(R - r)$ to r. This problem is avoided by using $|R-r|$ as the lower integration limit. On integrating, you obtain equation [8] the expression for the number of alpha particles escaping per second from the source sphere of radius r.

$$n = 4/3\ \pi r^3\ n_o \left[\frac{R}{16r}\left(12 - \frac{R^2}{r^2}\right)\right] \qquad [8]$$

Since the total alpha emission from the plutonium in a microsphere is $4/3\ \pi r^3\ n_o$, the fraction escaping (f) can be obtained by dividing equation [8] by this value. Therefore,

$$f = \frac{R}{16r}\left(12 - \frac{R^2}{r^2}\right) \qquad [9]$$

The mathematical test of this equation is its ability to meet the boundary condition that when $R = 2r$, then $f = 1$. This is intuitively necessary by the argument that if $2r \leq R$, all of the alpha particles must escape from the microsphere and the ratio of the effective activity to the total activity must be unity.

M. E. Anderson [9], assuming that the radius of the sphere of emission is so small compared to the radius of the microsphere that the surface of the microsphere is closely approximated by a flat surface, derived a simpler relationship:

$$f = 3/4\ \frac{R}{r} \qquad [10]$$

The derivation is nearly identical, but the integration is greatly simplified by the flat surface approximation. However, notice that at the boundary condition, $R = 2r$, $f = 1.5$ rather than unity as necessary. Comparison of equations [9] and [10]

shows that Kershner's equation has as its second term, the correction factor,

$$-\frac{1}{16}\left(\frac{R^3}{r^3}\right) \qquad [11]$$

which could only be significant when r approaches R. The critical nature of the relationship between r and R can be seen if f is plotted against r/R (Fig. 2).

During the study, proper interpretation of the alpha spectrum became a question of some concern. C. J. Kershner[8] derived a relationship based on a modified model suggested by Chudacek[35] (see Fig. 3). The incremental number of alpha particles, dn_x, emitted per unit area through a point P on the surface of a sphere of radius r from a distance x below the surface and originating from an incremental volume $2\pi x^2 \sin\varphi d\varphi dx$, is

$$dn_x = \frac{n_o K_1 2\pi x^2}{4\pi x^2}\int_0^{\cos^{-1}\left(\frac{x}{2r}\right)} \sin\varphi \; d\varphi \; dx. \qquad [12]$$

where n_o is the total number of alpha particles emitted per cubic centimeter and K_1 is a proportionality constant. The $4\pi x^2$ term in the denominator is required to normalize the flux at a distance x from a point source.

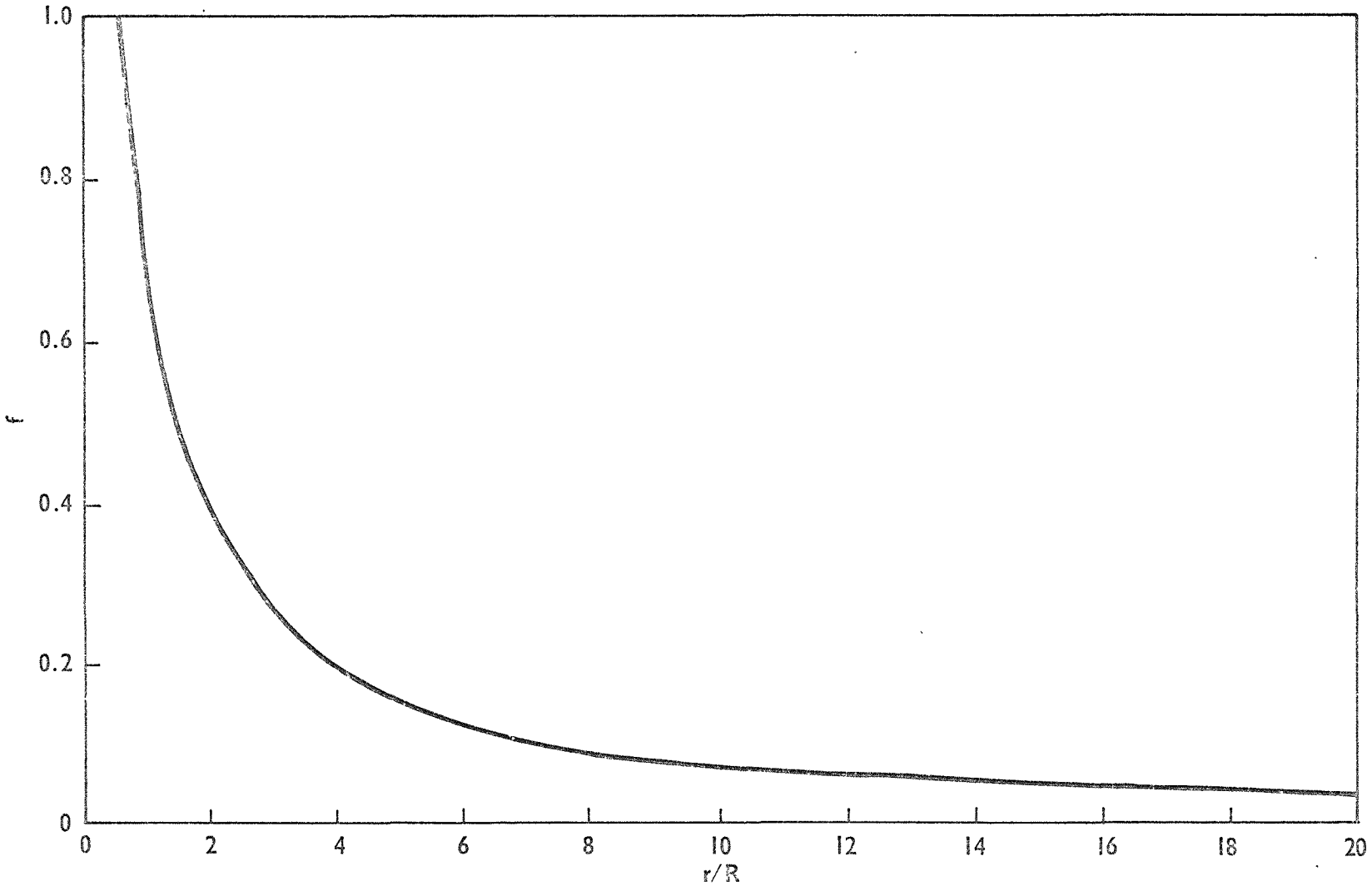
FRACTION (f) OF ALPHA PARTICLES ESCAPING
FROM A SOURCE SPHERE OF RADIUS (r)
1.0
0.8
0.6
0.4
0.2
0
f
0
2
4
6
8
10
12
14
16
18
20
r/R

FIGURE 2

MODEL FOR DERIVATION OF ENERGY SPECTRUM

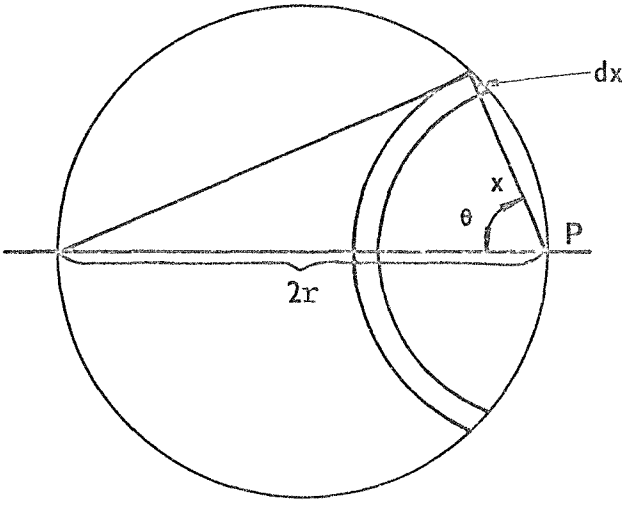

FIGURE 3

Integrating equation [12] after simplifying;

$$dn = - \frac{n_o K_1}{2} \left(1 - \frac{x}{2r}\right) dx. \qquad [13]$$

Since all of the points on the surface of the sphere are identical, equation [13] represents the number distribution of alpha particles being emitted as a function of path length in the source.

Using this model (Fig. 3), we can approximate a flat surface by allowing the radius to expand to infinity, i.e., let $r = \infty$. For a flat surface, the number of alpha particles emitted from all possible path lengths is equal and thus the energy spectrum of the escaping alpha particles emitted from all possible path lengths is equal and thus the energy spectrum of the escaping alpha particles is a function of the energy-path relationship only. This is only partially true for a sphere because the energy spectrum of a sphere is also a function of the radius, whose contribution logically becomes more important as the radius approaches the range of an alpha particle in the sphere.

The Geiger Rule[9] is an empirical energy-path relationship which allows one to correlate the variables discussed above. It is mathematically expressed as:

$$x = K_2 \left(E_o^{3/2} - E_x^{3/2}\right) \qquad [14]$$

where E_o is the initial kinetic energy, E_x is the kinetic energy at distance x, and K_2 is a proportionality constant. Taking the derivative of equation [14],

$$dx = - 3/2\ K_2\ E_x^{1/2} dE_x\ . \qquad [15]$$

Integrating dx from R to zero and dE_x from zero to E_o, it can be seen that

$$K_2 = \frac{R}{E_o^{3/2}} \qquad [16]$$

where R is the mean range (i.e., $R \equiv \bar{R}$) of an alpha particle. Substituting equations [14] and [15] into [13] and integrating dn from zero to n_E and dE from zero to E, one obtains

$$n_{o-E} = \frac{n_o K_1 K_2}{2} E^{3/2} \left\{1 - \frac{R}{2r}\left[1 - 1/2 \left(\frac{E}{E_o}\right)^{1/2}\right]\right\} \qquad [17]$$

Substituting equation [16] into [17] one obtains:

$$n_{o-E} = \frac{n_o K_1 R}{2} \left(\frac{E}{E_o}\right)^{3/2} \left\{1 - \frac{R}{2r}\left[1 - 1/2 \left(\frac{E}{E_o}\right)^{1/2}\right]\right\} \qquad [18]$$

where n_{0-E} is all of the alpha particles contributing to the spectrum between zero energy and kinetic energy E. Equation [18] has been solved and plotted (Fig. 4) for three cases. The first case is the flat surface approximation (i.e., where $r = \infty$),

$$n_{0-E} = \frac{3n_0 K_1 R}{4} \left(\frac{E}{E_0}\right)^{3/2} \qquad [19]$$

second, where $R = 3r$

$$n_{0-E} = \frac{n_0 K_1 R}{4} \left(\frac{E}{E_0}\right)^{3/2} \left[\frac{3}{2} \left(\frac{E}{E_0}\right)^{1/2} - 1\right] \qquad [20]$$

and third, where $R = 2r$

$$n_{0-E} = \frac{n_0 K_1 R}{4} \left(\frac{E}{E_0}\right)^{2} \qquad [21]$$

To simplify the plotting procedure, equations [19], [20] and [21] were normalized by obtaining the fraction (f) of the total number of alpha particles which n_{0-E} contribute to the spectrum,

$$f_{0-E} = \frac{n_{0-E}}{n_{0-E_0}} \qquad [22]$$

Then, the intensity of the contribution to the spectra of alpha particles between energy E_1 and E_2 was obtained by defining a quantity

$$\Delta f_{E_1-E_2} = f_{0-E_2} - f_{0-E_1} \qquad [23]$$

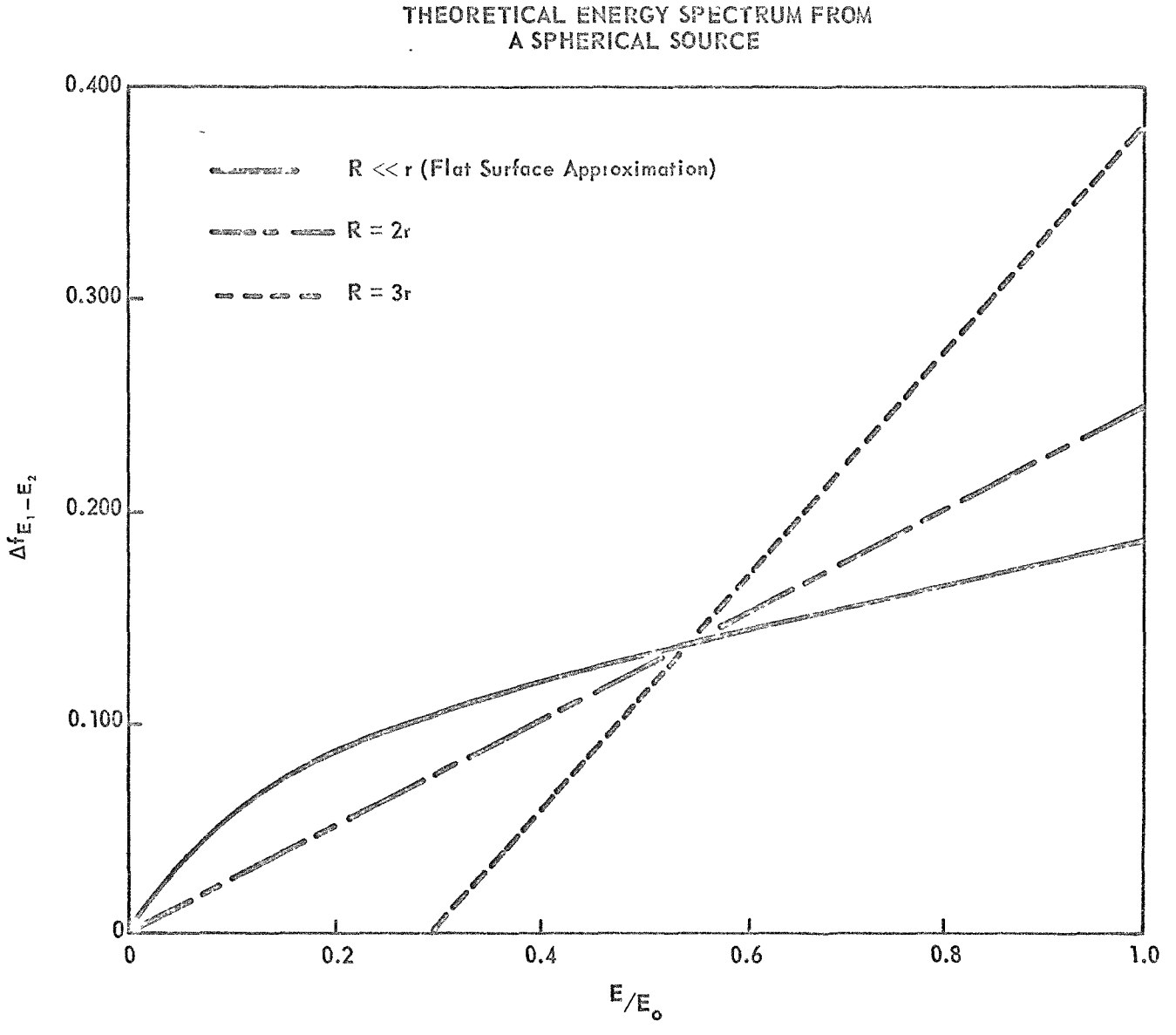

Note: Since the intensity function, $\Delta f_{E_1-E_2}$, is dependent on the energy interval chosen (see equations [19] through [24]), this scale is completely arbitrary. For the valves plotted above, $E_2-E_1 = 1/8\ E_o$

FIGURE 4

The values obtained from equation [23] were plotted (Fig. 4) against the values obtained from equation [24] which is the average energy E_A for the energy interval from E_1 to E_2 which is expressed mathematically as:

$$E_A = \frac{E_1 + E_2}{2E_o} \qquad [24]$$

As the radius decreases, that is as the relationship R/r increases in magnitude, the spectrum will continue to shift towards the vertical line until the spectrum becomes a vertical line. Such a case is the theoretical spectrum for a very thin sample.

EXPERIMENTAL

I. Instrumentation

A glovebox (Fig. 5) was especially designed for this study. It is constructed of plexiglas and incorporates the following systems:

1. An American Optical Microstar Series 10 Microscope with objectives allowing photomicrographs of 40X and 100X,

2. A Cahn Model G Gram Electrobalance with external controls,

3. Two Zeiss Micromanipulators mounted on turntables with an external pressure-vacuum pump,

4. An Ortec model 804 vacuum counting chamber with a silicon surface barrier detector and an external vacuum system.

External to the glovebox is a lithium drifted germanium detector of the coaxial type. Both detectors feed into the same 256 - channel analyzer through the standard electronic components shown diagrammatically (Figs. 6 and 7).

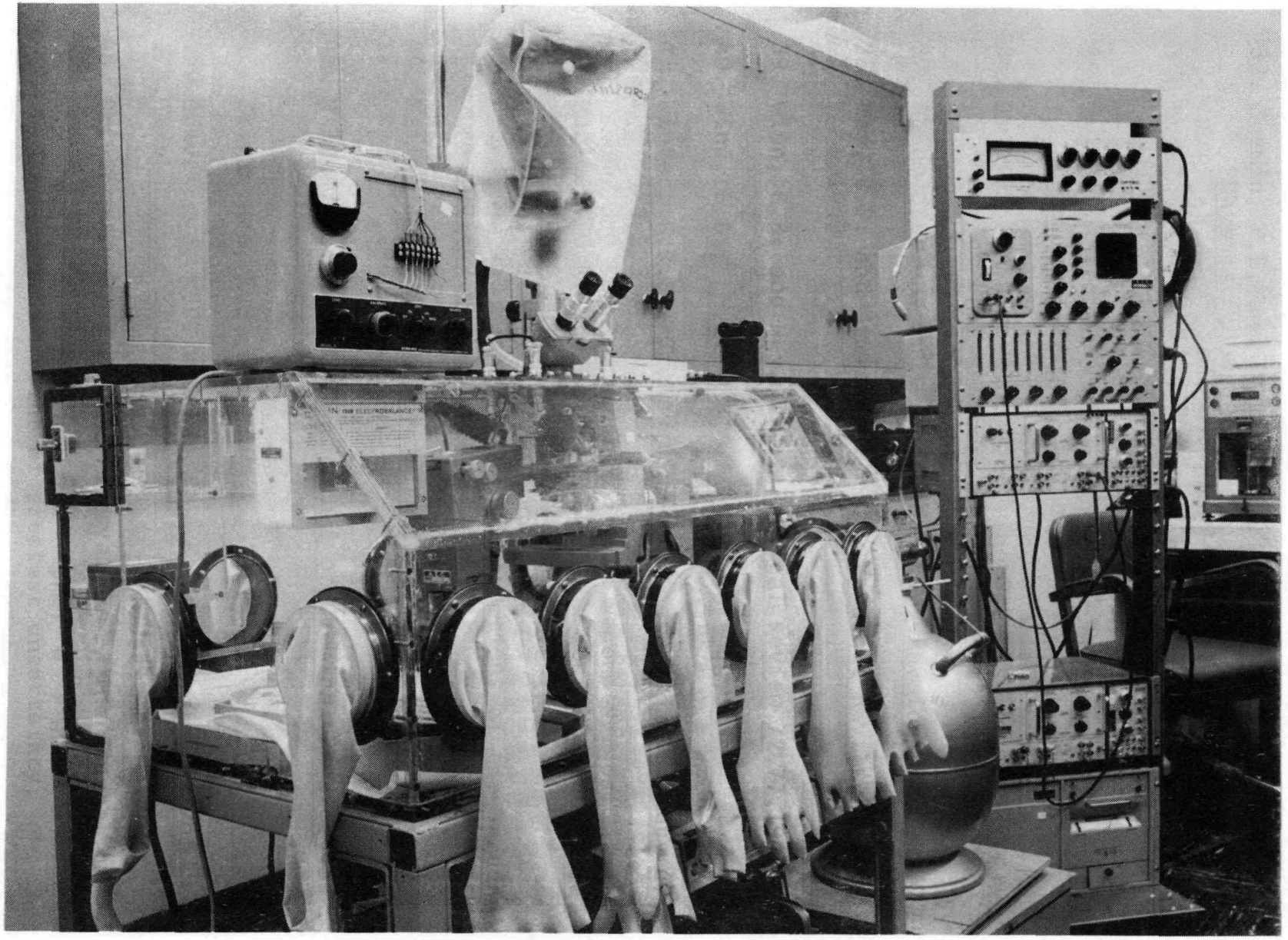

FIGURE 5: THE EXPERIMENTAL ARRANGEMENT

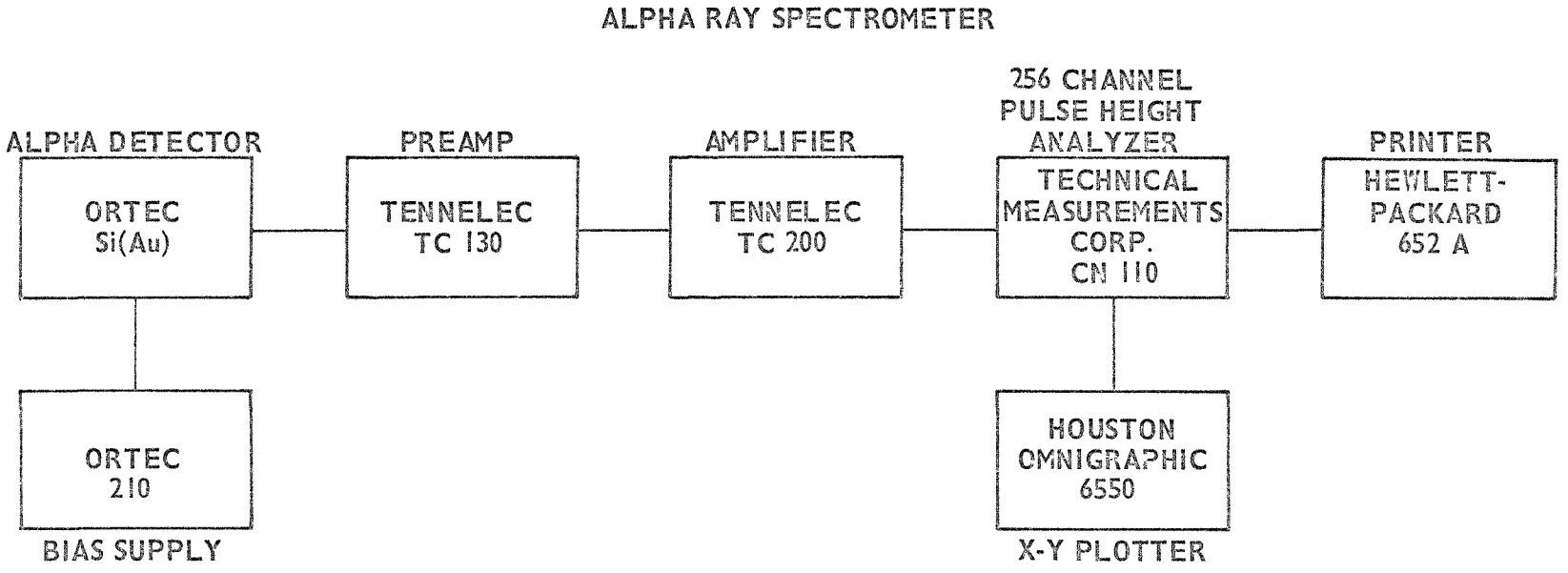
ALPHA RAY SPECTROMETER
ALPHA DETECTOR
ORTEC
Si(Au)
PREAMP
TENNELEC
TC 130
AMPLIFIER
TENNELEC
TC 200
256 CHANNEL
PULSE HEIGHT
ANALYZER
TECHNICAL
MEASUREMENTS
CORP.
CN 110
PRINTER
HEWLETT-
PACKARD
652 A
ORTEC
210
BIAS SUPPLY
HOUSTON
OMNIGRAPHIC
6550
X-Y PLOTTER

FIGURE 6

GAMMA RAY SPECTROMETER

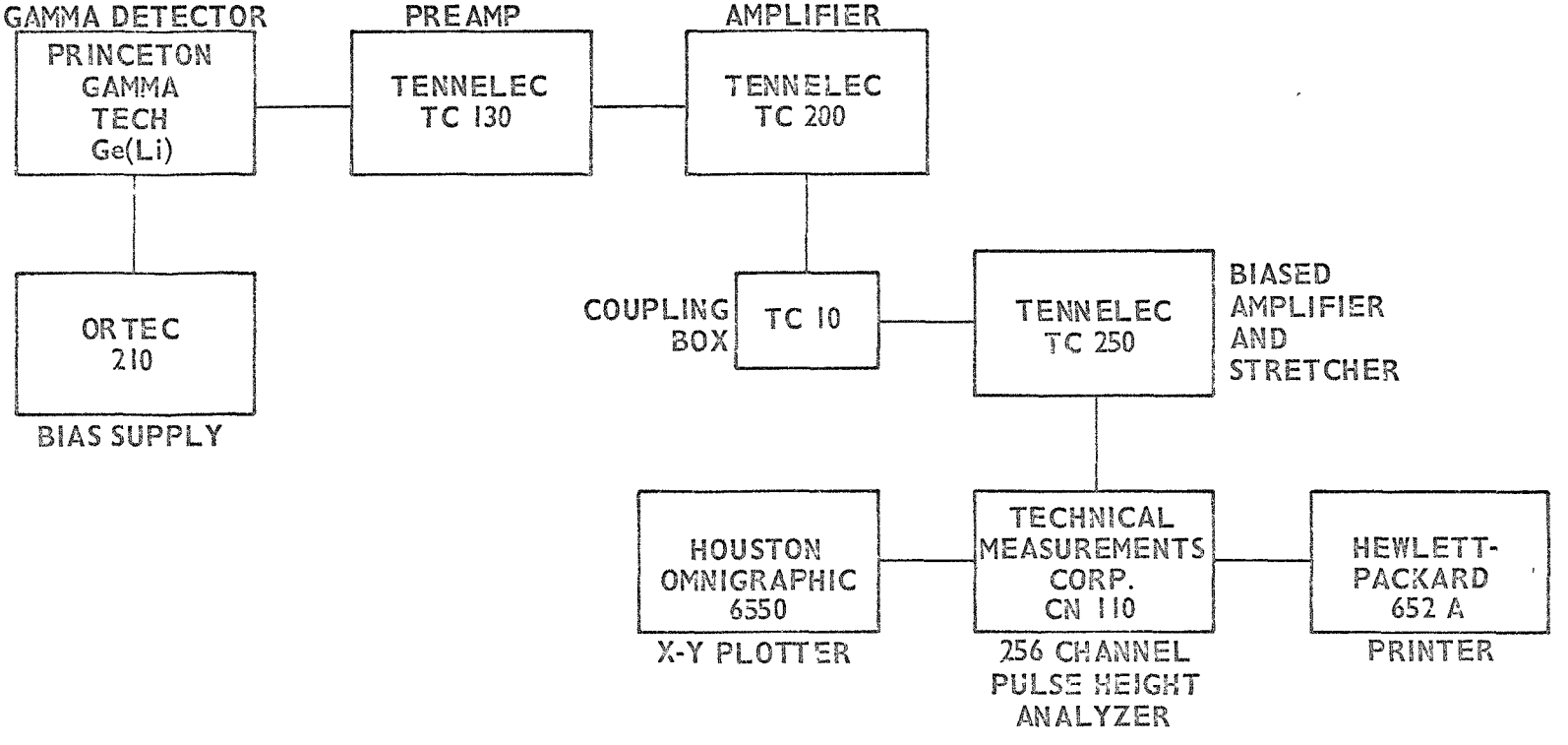

FIGURE 7

The only unusual aspect of this glovebox is the micromanipulators which allow the selection of a specific particle from the midst of hundreds of particles of similar size and shape. For example, selection of sample 2 was made from approximately 200 microspheres ranging in size from 130 μm to 170 μm in diameter. The micromanipulators are mounted on turntables to allow for easy movement of the manipulators in and out of the field of the microscope. The left hand manipulator (Fig. 8) is aligned with the counting planchet of the Ortec counter as well as the microscope stage. This allows small microspheres to be selected from the microscope stage (less than 100 microns in diameter) and centered on the counting planchet of the Ortec counter. A 40x microscope is positioned by the Ortec counter for use in such instances (Fig. 9).

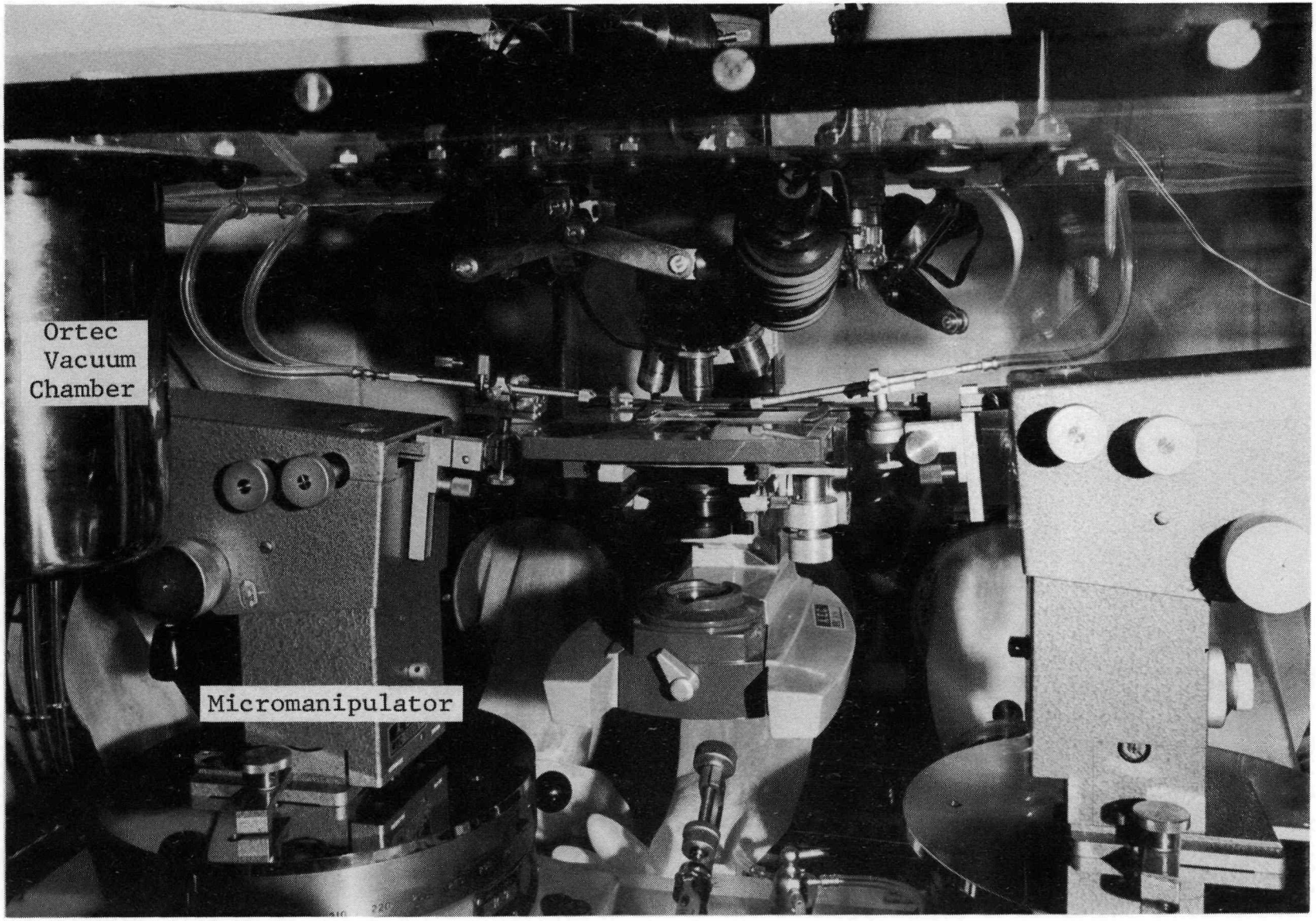

FIGURE 8: THE LEITZ MICROMANIPULATORS

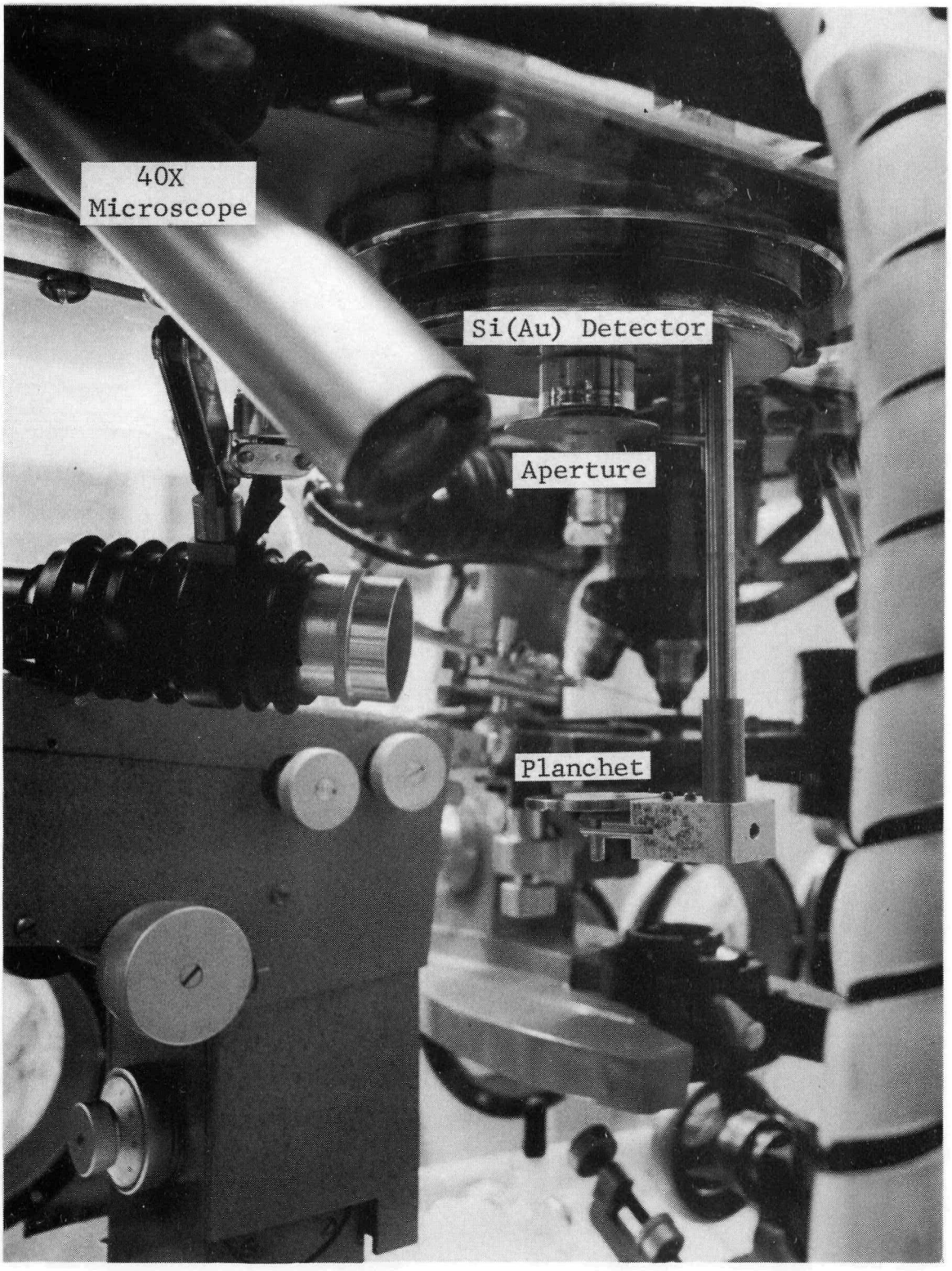

FIGURE 9: INTERIOR OF THE ORTEC COUNTING CHAMBER

II. Sample Selection

It was decided that the plutonium-238 dioxide microsphere samples used in this study should be prepared from microspheres produced by a group at Mound Laboratory[10] studying the sol-gel process developed by Oak Ridge.[11],[12] Experience has shown that sol-gel microspheres are especially suited to this study because they tend to have densities near the maximum theoretical value of 11.46 gm cm^{-3}[13] which implies little or no voids and a uniform density throughout the microsphere. Also, they have relatively high crush strengths and less tendency to release submicroscopic contaminants. The crush strength is the mass in grams required to crush a single plutonium-238 dioxide microsphere.

An alternative was to use plutonium-238 dioxide microspheres being produced on a large scale by passing dense plutonium-238 dioxide powder through a plasma torch.[14] These microspheres have densities in the range 9.8-10.4 gm cm^{-3}[13] which reflects the fact that they have numerous or large voids and are usually non-uniform in density. The major reason for excluding their

use, however, is their tendency to release submicroscopic contaminants which readily become airborne and would contaminate the glovebox and Ortec counter. This is compounded by their relatively low crush strengths which, if a particle were crushed, would result in extensive contamination.

Sample 1 was prepared from sol-gel batch 102. The batch was washed alternately with Thompson's Blue Glass Cleaner and absolute ethanol until a 5 ml rinse of absolute ethanol was judged to be free of plutonium contamination. This same procedure was followed in cleaning subsequent batches and in each case the test was repeated twice to confirm the batch was free from loose contamination.

After cleaning, the batch was passed through six sieves in the range from 30 μm (micrometers) to 300 μm. The loose fraction collected in each sieve was discarded and each sieve was inverted and tapped once sharply to release any particles loosely held in the mesh of the sieve. The remaining particles were assumed to be of diameters in close approximation of the tolerances of the sieve openings. These microspheres were collected by forcing the particles out of the sieve openings with an artist brush. The intention was to obtain about ten microspheres of exactly the same diameter in each sieve range.

Microscopic examination of the six samples obtained above showed that the statistical mode in each sample was 150 μm for the diameters of the microspheres. This was unexpected in view of earlier work[15] for which this type of sample preparation had been successful. It could only be assumed, that although the sieves were new and previously unused, the batch was of a very narrow diameter distribution and with the exception of an insufficient quantity of microspheres within the tolerances of each sieve, there must be a large number of sieve openings in the range of 150 μm to collect this modal distribution. Sample 1 was then prepared by selecting ten microspheres of approximately 150 μm in diameter (Fig. 10).

Preparation of sample 1 revealed several problems. First, the unpredictable electrostatic attraction toward and repulsion from the glass microtool of the micromanipulator made loss of microspheres difficult to prevent. Second, electrostatic attraction of the microspheres toward foreign material resulted in an agglomeration of this material on the surface which could not be tolerated if their effective activities were to be determined. Third, it appeared that especially for smaller microspheres (i.e., 150 μm in diameter and less) the design of the microtool is critical. Many times a microsphere could not be picked up or it could not be set down once it was picked up.

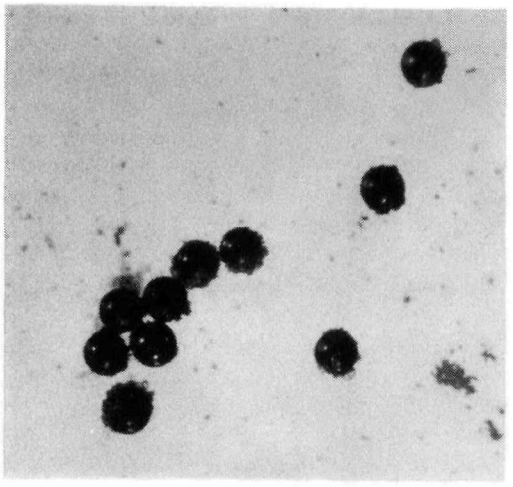

FIGURE 10: SAMPLE 1 (40X)

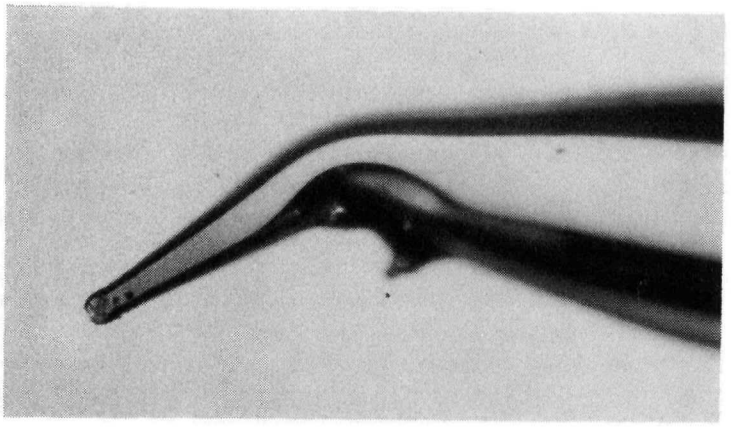

FIGURE 11: TIP OF A MICROTOOL (40X)

Also many microtool designs allowed excessive force to be placed on the microsphere, with the result that it would jump away from the microtool, many times resulting in the loss of the microsphere.

In spite of the fact that Sample 1 had excessive amounts of agglomerated material adhering to the surface after several attempts at cleaning and could not be used in this study, enough information was obtained from Sample 1 to make the preparation of subsequent samples feasible. The agglomerated surface contaminate was determined to be primarily talcum powder and was subsequently reduced by washing all gloves before using them on the glovebox. The handling problems were controlled in two manners. First, the water content in the air of the box was reduced by placing open dishes of phosphorous pentoxide in the glovebox and the microsphere samples and microtools were allowed to stand open in close proximity to the phosphorous pentoxide. This had the effect of reducing the static problem to a useful level. Under these conditions a microsphere could be easily manipulated and once it was placed on a glass or metal surface for a few seconds it developed enough static attraction to hold it in position. This was a very useful property since it prevented loss of

the microspheres while evacuating the Ortec counting chamber. Second, the static effect was further reduced by always manipulating the microspheres under absolute ethanol. That is, one or two drops of ethanol was placed over the microsphere to be picked up by the microtool and one or two drops of ethanol were placed on the surface to receive the microsphere to facilitate its release from the microtool.

The loss of microspheres due to excessive pressure from the microtool was reduced by the ethanol cover technique, but it was primarily controlled by an optimum design of the microtool (Fig. 11). It was found that if the tip of the microtool was angled 45° from the shaft and if the cup were 2/3 the diameter of the microsphere (especially for microspheres 150 μm diameter and less) microsphere loss could be reduced and problems like excessive static attraction or repulsion, wedging, or insufficient suction could be controlled. Henceforth, all necessary microtools were prepared to these specifications with a DeFonbrune Microforge and Leitz needle puller (Fig. 12) using standard techniques, and with the exception of the special techniques just discussed, all manipulation was conducted with standard techniques.[16]

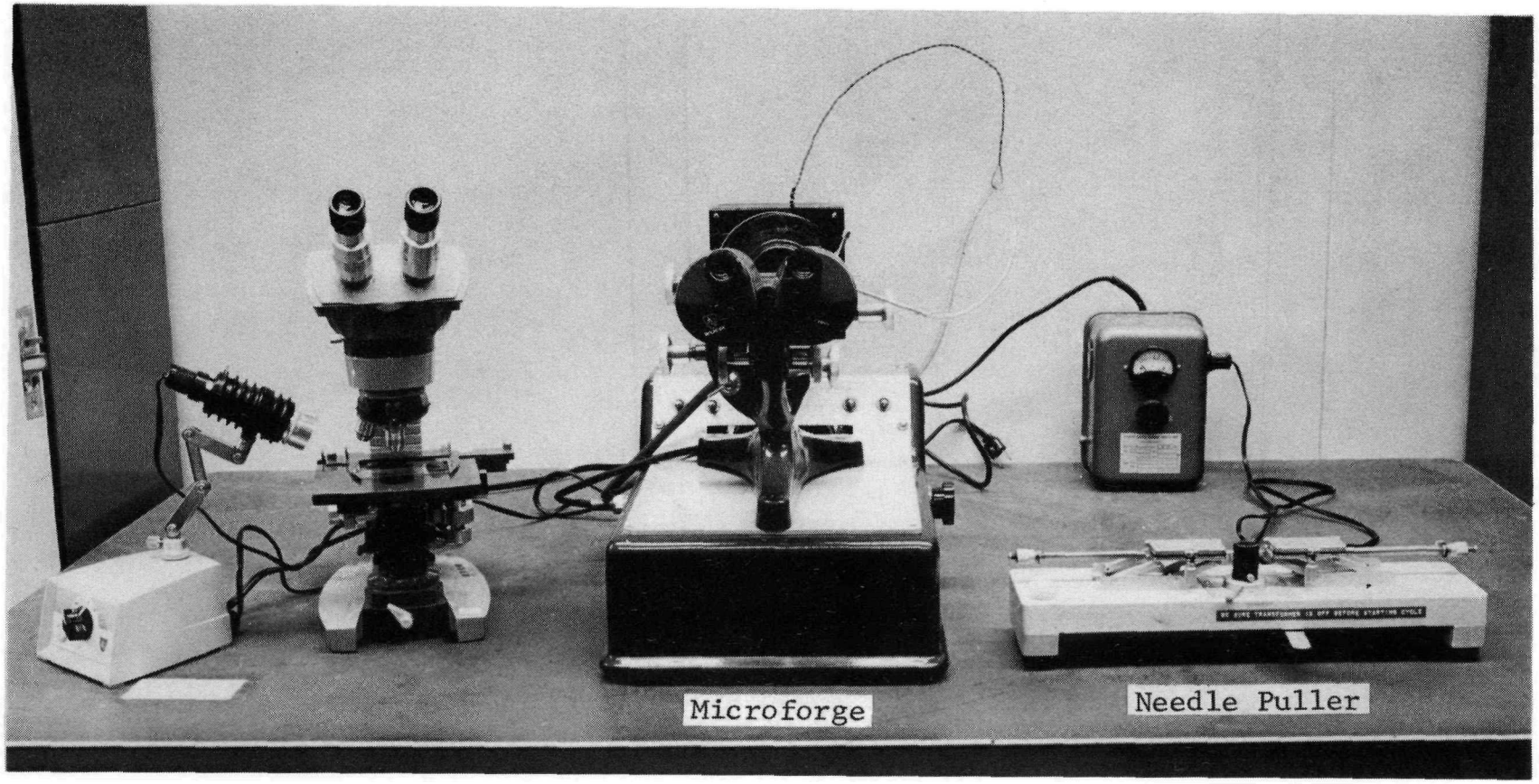

FIGURE 12: DEFONBRUNE MICROFORGE AND LEITZ NEEDLE PULLER

It should be noted that the experience with Sample 1 showed the impossibility of collecting ten microspheres of exactly the same diameter. Therefore, an attempt was made to prepare the subsequent samples over a diameter interval not exceeding 10 μm from the smallest to the largest microsphere in the sample. Sample 2 was prepared from the original sol-gel batch 102, Sample 3 from sol-gel batch 425 and Sample 4 from sol-gel batch 505. The samples were prepared by placing a few microspheres at a time on a slide and selecting as many microspheres near the desired size and as close to each other in diameter as possible. Fortunately, the mode of each sample was approximately 150, 200, and 250 μm respectively, which was convenient for this study. The success of the above techniques in reducing the contamination of the samples by foreign materials can be seen by comparing Samples 2, 3, and 4 (Fig. 13) with Sample 1 (Fig. 10).

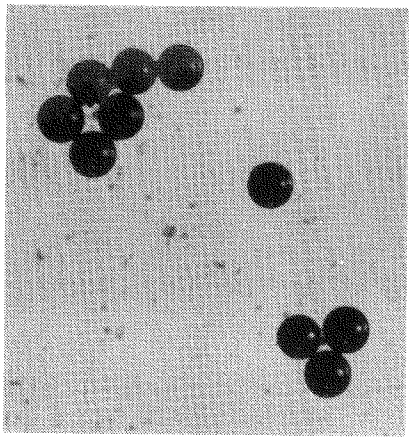

SAMPLE 2

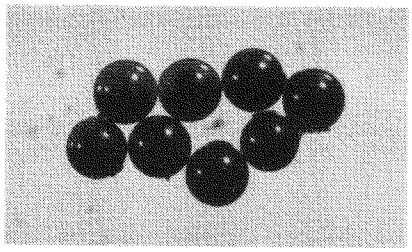

SAMPLE 3

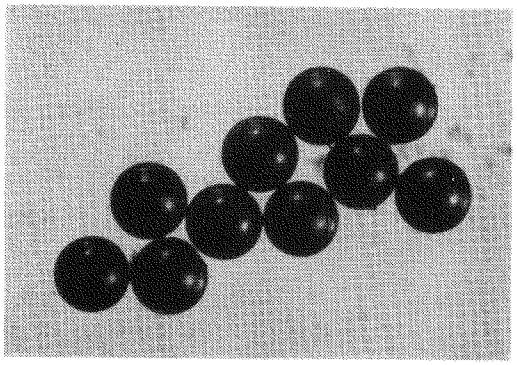

SAMPLE 4

FIGURE 13: SAMPLES 2, 3, and 4

III. Weighing Procedure

The balance used for weighing the microsphere samples was calibrated on the 1, 5, and 10 mg (milligram) scale using standard weights prepared by the Mass Standards Department at Mound Laboratory. The balance was found to be extremely linear, but slightly inaccurate. Since only the 1 mg scale was used in weighing the samples, it is the only one for which the calibration results are given here. Table 1 shows a least squares analysis of a plot of the experimentally determined weight ($X_{obs.}$) versus the actual weight ($Y_{act.}$). A new weight ($Y_{calc.}$) is calculated by the method of least squares for each experimental weight and the slope (m) and intercept (b) is given for the line defined by these Y values. With the slope and intercept values we can now calculate the weight of an unknown particle from its experimentally observed weight using an equation of the form;

$$y_{calc} = mx_{obs} + b$$

TABLE 1

LEAST SQUARES FIT TO THE CALIBRATION DATA FOR THE ONE MILLIGRAM BALANCE SCALE

$X_{obs.}$ Experimental Weight[a]	$Y_{act.}$ Actual Weight[b]	$Y_{calc.}$ L.S. Calculated Weight	Residuals
0.503500	0.5029900	0.5028428	+0.0001472
0.305500	0.3045600	0.3077734	-0.0002134
0.218000	0.2170700	0.2172427	-0.0001727
0.123100	0.1225400	0.1223095	+0.0002305
0.043600	0.0427900	0.0427816	+0.0000084

Slope (m) 1.00035
Y Intercept (b). . . . . 8.33701×10^{-4}

Standard Error of Estimate (σ) -- 0.000173

$$\text{where } \sigma = \sqrt{\frac{\Sigma(\text{Residuals})^2}{n}}$$

[a] The experimental weight is actually calculated according to the formula $X_{cls.}$ = (percent of full scale) x (1.0016 mg) where the balance was calibrated using a 1.0016 mg weight at full scale.

[b] The possible inaccuracies in the calibrated weights is reported as ± .0025 mg but is actually three times better.

and it is assumed that the calculated weight is closer to the true value than the experimentally observed value. Support for this assumption is seen by observing the residuals in Table 1. The largest deviation from the Mass Standards value is 0.23 μg.

As each sample was prepared it was transferred to a weighing pan by placing two drops of absolute ethanol in the weighing pan and using a rubber-tipped stirring rod slightly moistened with ethanol to pick up the microspheres. As soon as the microspheres contacted the ethanol in the weighing pan they dropped free from the policeman. The pan was then placed on the balance. All of the ethanol was assumed to have evaporated when the weight stabilized.

After obtaining the weight of an entire sample, the weighing pan was returned to the microscope stage where the micromanipulator was used to remove one microsphere. The removal of microspheres from the weighing pan by the micromanipulator was the only manipulation procedure that was carried out dry. This was necessary because each drop of ethanol contained approximately 90 μg of a chemical impurity. However, the spherical bottom of the weighing pan made the probability of applying excessive pressure to the microsphere negligible and this

procedure could be carried out with a low probability of sample loss. After a microsphere was removed, the pan was returned to the balance and allowed to stabilize while the microsphere just removed was photographed using standard photomicrographic techniques.[18] This process was repeated until all of the microspheres were weighed, photographed, numbered and individually packaged. Then the empty pan was weighed to determine the weight of the ethanol residue. A stage micrometer was photographed before Sample 2 and after Sample 4 to be sure that no mechanical changes in the microscope were effecting the magnification at the film plane. No change was observed.

The diameters of the microspheres were taken as the average of three diameter measurements on the negatives of the individual photomicrographs (Figs. 14, 15 and 16) taken at 120° from each other where obvious bumps or flats were purposely avoided. This means that the average diameters shown in Tables 2, 3 and 4 are the apparent spherical diameters for a single view of the microspheres and any obvious flats or bumps on the surface have not been considered in diameter and volume calculations. From experience, the contribution of such surface deformities on microspheres in the size range studied is negligible. Since it was beyond the scope of this study to view the microsphere

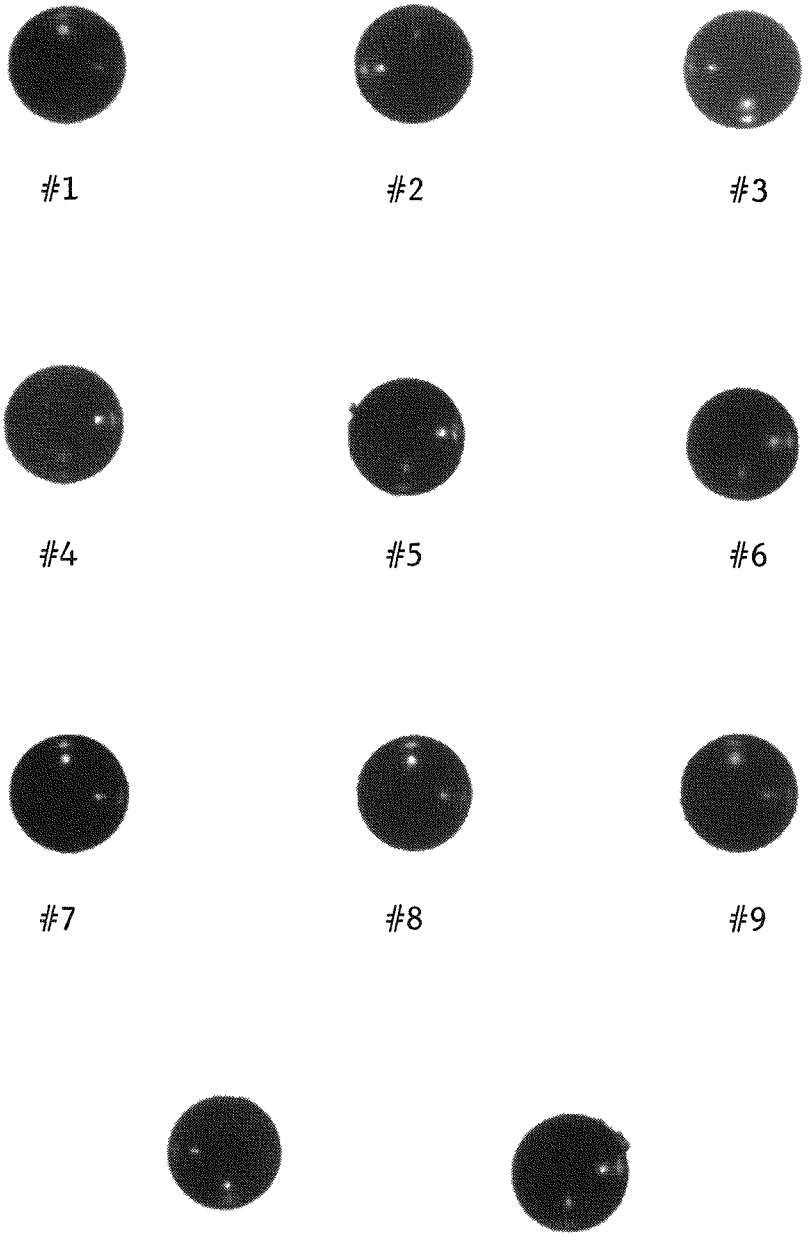

FIGURE 14: INDIVIDUAL MICROSPHERES IN SAMPLE 2

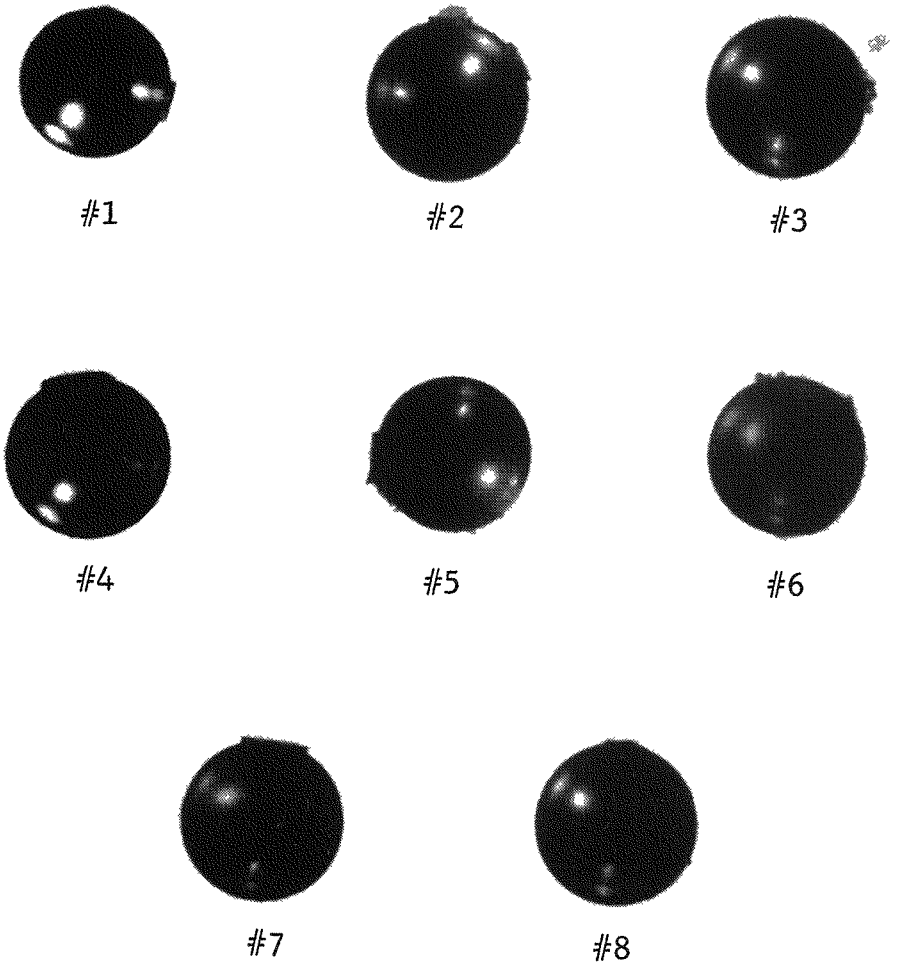

(Mag.: 100X)

FIGURE 15: INDIVIDUAL MICROSPHERES IN SAMPLE 3

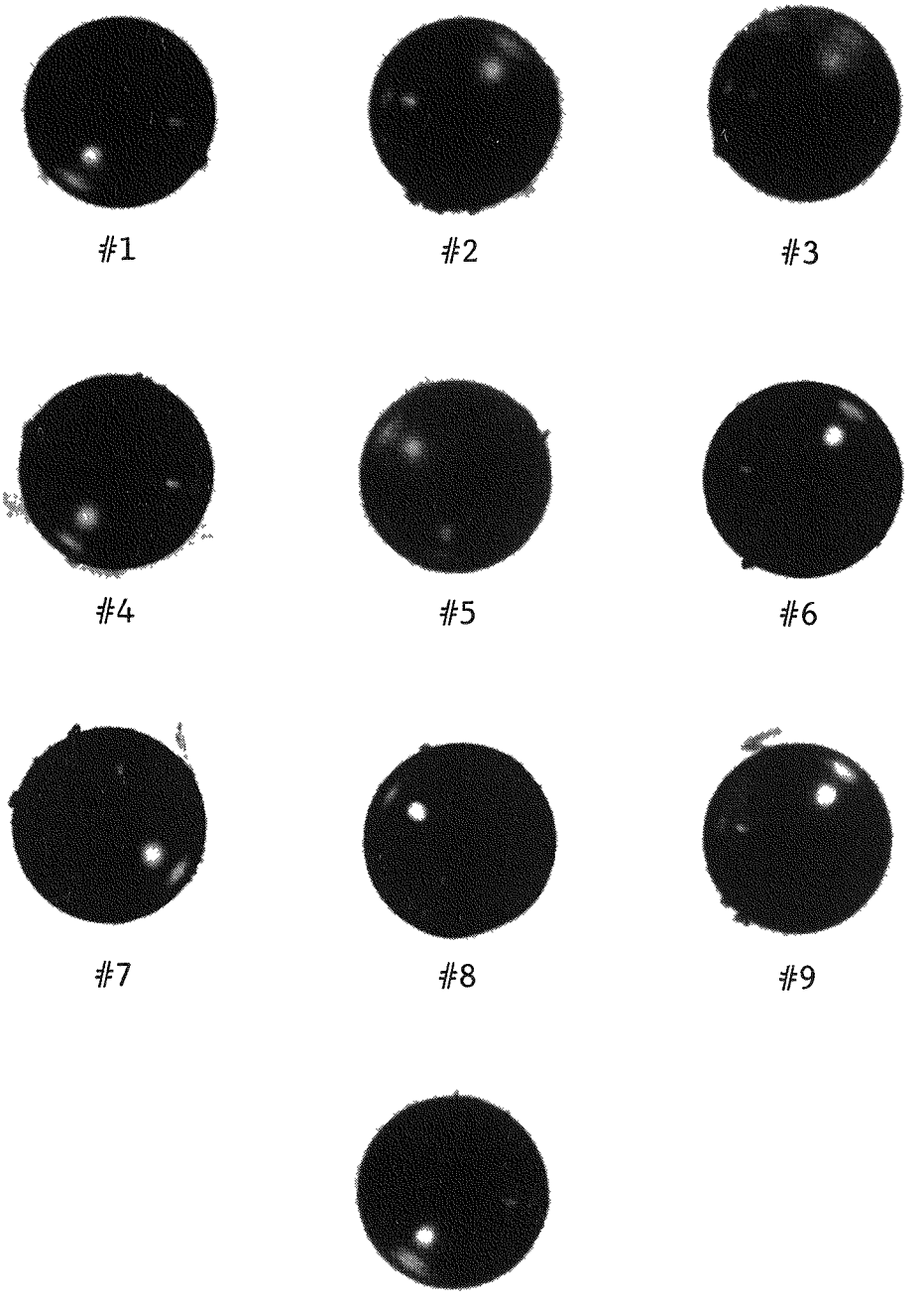

(Mag.: 100X)

FIGURE 16: INDIVIDUAL MICROSPHERES IN SAMPLE 4

TABLE 2

DIAMETER, WEIGHT, AND CALCULATED DENSITY DATA FOR SAMPLE 2

Microsphere Ident. No.	Diameter ± σ in Microns	Weight in Micrograms	Calculated Density gm cm^{-3}
1	153.1 ± 0.2	20.2	11.02
2	153.8 ± 0.3	19.9	11.05
3*	154.2 ± 0.4	21.4	11.12
4	154.1 ± 0.4	20.8	11.12
5	151.6 ± 0.0_7	21.2	11.16
6*	145.7 ± 0.3	17.8	11.08
7*	153.1 ± 0.2	20.7	11.09
8*	149.4 ± 0.2	19.4	11.11
9	152.9 ± 0.3	22.0	11.11
10	147.0 ± 0.0_7	17.6	10.77
11	152.5 ± 0.0_3	20.3	10.93

Average Density For Sample 2 . . . . 11.05 ± 0.11

*These microspheres were used later in the alpha counting procedure.

TABLE 3

DIAMETER, WEIGHT AND CALCULATED DENSITY DATA FOR SAMPLE 3

Microsphere Ident. No.	Diameter ± σ in Microns	Weight in Micrograms	Calculated Density gm cm^{-3}
1	193.7 ± 0.2	39.3	11.02
2	208.7 ± 0.1	52.5	11.11
3*	208.1 ± 0.0_5	52.1	11.12
4	209.8 ± 0.3	52.8	11.17
5	200.9 ± 0.4	48.3	11.19
6	205.4 ± 0.2	50.8	11.13
7*	208.4 ± 0.0_5	52.9	11.10
8*	211.2 ± 0.1	54.5	11.05

Average Density for Sample 3 . . . . 11.11 ± 0.05

*These microspheres were used later in the alpha counting procedure.

TABLE 4

DIAMETER, WEIGHT, AND CALCULATED DENSITY DATA FOR SAMPLE 4

Microsphere Ident. No.	Diameter ± σ in Microns	Weight in Micrograms	Calculated Density gm cm^{-3}
1*	248.3 ± 0.3	89.3	11.11
2	249.2 ± 0.6	89.8	11.11
3	252.6 ± 0.7	93.4	11.11
4	253.6 ± 0.8	96.4	11.12
5	250.7 ± 0.3	91.5	11.09
6*	256.3 ± 0.5	96.7	11.09
7	251.5 ± 0.0	92.9	11.12
8	250.8 ± 0.4	89.6	11.11
9*	248.2 ± 0.6	91.0	11.25
10*	250.8 ± 0.5	92.0	11.14

Average Density for Sample 3 . . . . 11.12 ± 0.04

*These microspheres were used later in the alpha counting procedure.

from other specific views with respect to that photographed, the assumption was made that the apparent spherical diameter and its associated calculated volume are accurate enough for this work.

Tables 2, 3, and 4 compile the results for the weighing procedure for Samples 2, 3 and 4 respectively. The diameters were calculated from the Dimensional Standards data given in Tables I, II, and III, Appendix A. The individual microsphere weights are the by difference weights between the final $y_{calc.}$ values which were derived as previously outlined. The density values given are not the densities for the individual microspheres. Rather, it is the average density for the microsphere opposite it in the table and all those below it in the table based on their experimentally determined weights and calculated volumes using the relationship:

$$\text{Volume} = \pi/6 \times (\text{diameter})^3$$

The theoretical density of plutonium-238 dioxide microspheres is 11.46 gm/cm^3.[13]

IV. Gamma Counting and Calorimetry Procedure

Following the weighing procedure, each microsphere was ready for gamma counting because they had been individually packaged on dimple microscope slides. In the short period prior to gamma counting and after the weighing procedure, the microspheres had had a chance to "stick" to these slides. This natural phenomena is the result of an electrostatic attraction and radiolysis effect whereby it is said that the microsphere "burns" its way into the surface of the glass slide. Microscopic examination has never shown any damage to the microsphere by this effect, and it makes for convenient handling of the microspheres.

To effect the gamma counting (Fig. 17), a piece of household saran wrap was placed over a gloveport and a Princeton Gamma Tech 12 cubic centimeter coaxial lithium drifted germanium detector was centered in contact with the saran wrap outside the glovebox.

DIAGRAM OF THE GAMMA COUNTING
SAMPLE ARRANGEMENT

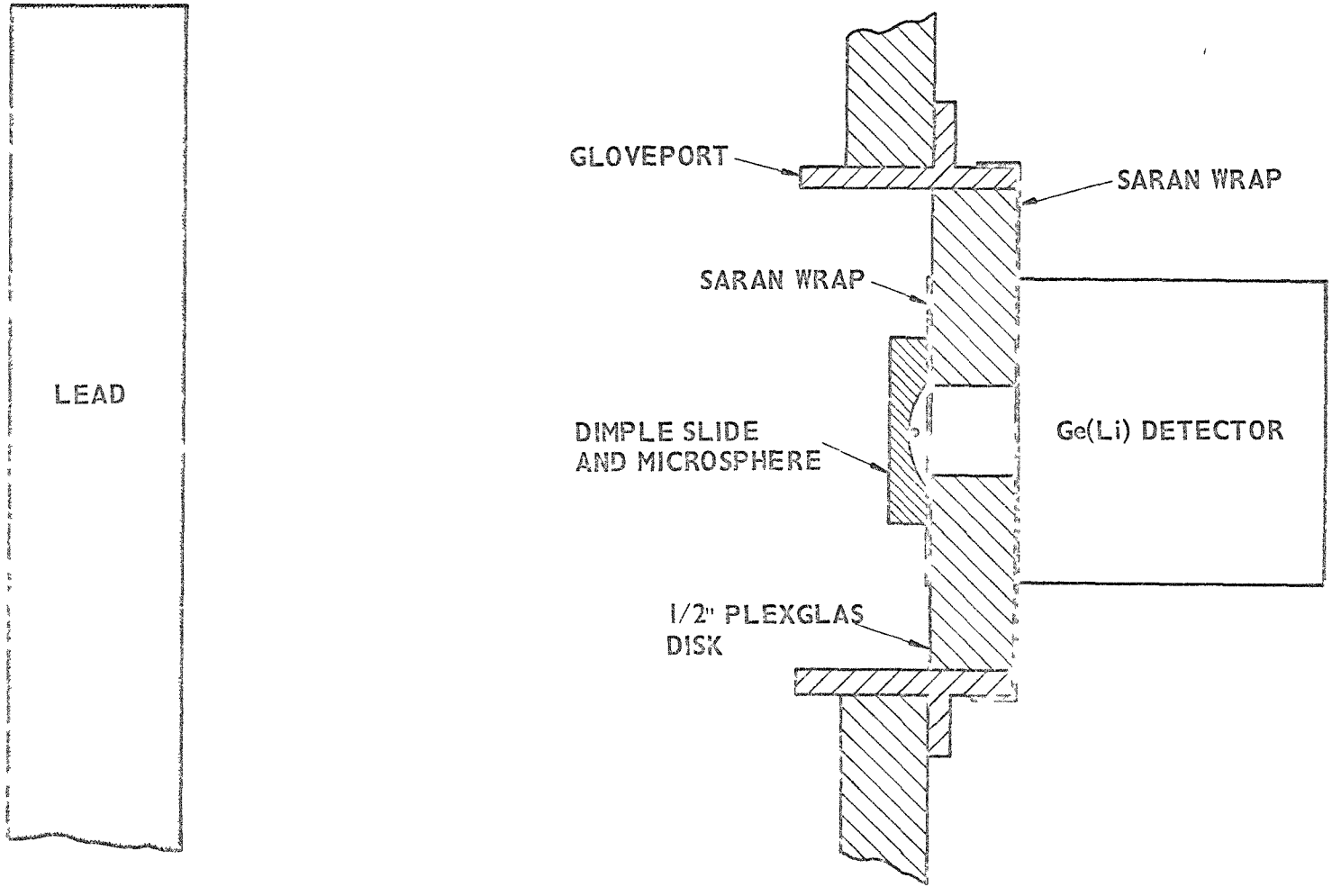

FIGURE 17

A round piece of half-inch thick plexiglass with a half-inch diameter hole drilled through it was fitted inside the glove-port with the hole centered on the face of the gamma detector and in contact with the detector through the saran wrap. The purpose of the plexiglass was to provide an easy means of reproducibily positioning each microsphere for gamma counting. Another piece of saran wrap was placed over the hole in the plexiglass disk to prevent accidental loss of a microsphere. The slide, with the microsphere sticking to it, was taped to the plexiglass disk so that the microsphere was positioned over the center of the hole.

Table 5[19] lists the various gamma radiations of plutonium-238. The fact that the 99.8 Kev gamma peak was counted in this study was primarily the result of balancing the availability of equipment against such factors as the energy of the various peaks. The lower energy radiations are more prone to self-absorption. There were two types of Ge(Li) detectors available for this study, the planar and coaxial. Ge(Li) detectors are especially good for counting the 99.8 Kev gamma peak of plutonium-238. The coaxial detector was chosen because while its efficiency is considerably lower than a planar detector, its resolution is better. In this study, the resolution of the 99.8 Kev

TABLE 5

ALPHA AND GAMMA RADIATIONS OF PLUTONIUM-238

Gamma Energy (Kev)	Photons $watt^{-1}$ sec^{-1} (calc.)
767	$\sim 5 \times 10^{5}$
203	4.4×10^{4}
153.1	1.0×10^{7}
99.8	9×10^{7}
43.5	4.2×10^{8}
17 (x-ray)	1.5×10^{11}
Alpha Energy (Mev)	**Particles $watt^{-1}$ sec^{-1} (calc.)**
5.491	7.95×10^{11}
5.448	3.20×10^{11}
5.352	1.5×10^{9}
5.200	5×10^{7}
5.000	7×10^{4}
4.700	1.3×10^{6}

gamma peak for the coaxial Ge(Li) detector was approximately 3.9 Kev Full Width at Half Maximum (FWIM) as opposed to 4.3 Kev FWHM for the planar detector. One requirement of this phase of the study was that the gamma counting be highly reproducible, i.e., very precise. Even though efficiency was sacrified, the better resolution of the coaxial detector increased the precision of the counting.

The object in gamma counting was to determine precisely the relative amounts of plutonium in the microspheres of a single sample. For Sample 2 which consisted of microspheres of 150 μm nominal diameter, a difference of one micron in diameter reflects a difference of approximately 2% in volume between the microspheres. However, for Sample 4, with a nominal diameter of 250 μm, a difference of one micron between two microspheres reflects a difference of only 1% in volume between the microspheres. Thus, it was desirable to collect more counts for the larger diameter microspheres in order to increase the precision of the data, but their larger volumes made this relatively easy. In the final analysis, the problem was to balance a reasonable counting time against a reasonable number of counts. The compromise reached was to count each microsphere in Sample 2 for 400 minutes, each microsphere in Sample 3 for 300 minutes, and each microsphere in Sample 4

for 200 minutes. Either immediately before or after each microsphere was counted, a 200 minute background was run. The result was over 100,000 counts under the 99.8 Kev peak of the microspheres in Sample 2 and over 200,000 counts under the peak of the microsphere in Sample 4.

Even though only one count was made of each sample, the precision of the count can be estimated by the knowledge that a spectral peak approximates a Poisson distribution[20] and as such, the standard deviation, σ, for an average of several determinations, $\bar{s}$, can be defined as

$$\sigma = \sqrt{\bar{s}}$$

and where a large number of counts is obtained, it may be assumed that, s, the number of counts in a single determination is approximately equal to the mean value, $\bar{s}$, and it can be assumed that

$$\sigma \simeq \sqrt{s}$$

Thus, where it is desired to detect a smaller difference in the amount of plutonium in plutonium dioxide microspheres, more counts are required.

It was discovered during a period of testing the counting procedure that the gamma counting could not be done during normal working hours at the laboratory. This was due to line voltage fluctuations from heavy use of electrical equipment during normal working hours and an unstable gamma background due to the movement of plutonium in other laboratories which could not be completely shielded out. Therefore, all of the gamma counting was done during the non-working periods at the laboratory.

Since the gamma background could not be controlled, a great many methods for the analysis of the gamma counting data were tried. The spectra shown (Fig. 18) is typical of the gamma counting data. The background spectra (Fig. 19) is also typical. Note that the peak channel (channel 67) is also clear in the background spectra.

A series of counts were made on microsphere #3 of Sample 4. In order that a method for integrating the area under the peak be acceptable, it was decided that it must meet the criteria that the standard deviation for the series of counts must not exceed the theoretical standard deviation (i.e., the square root of the mean value).

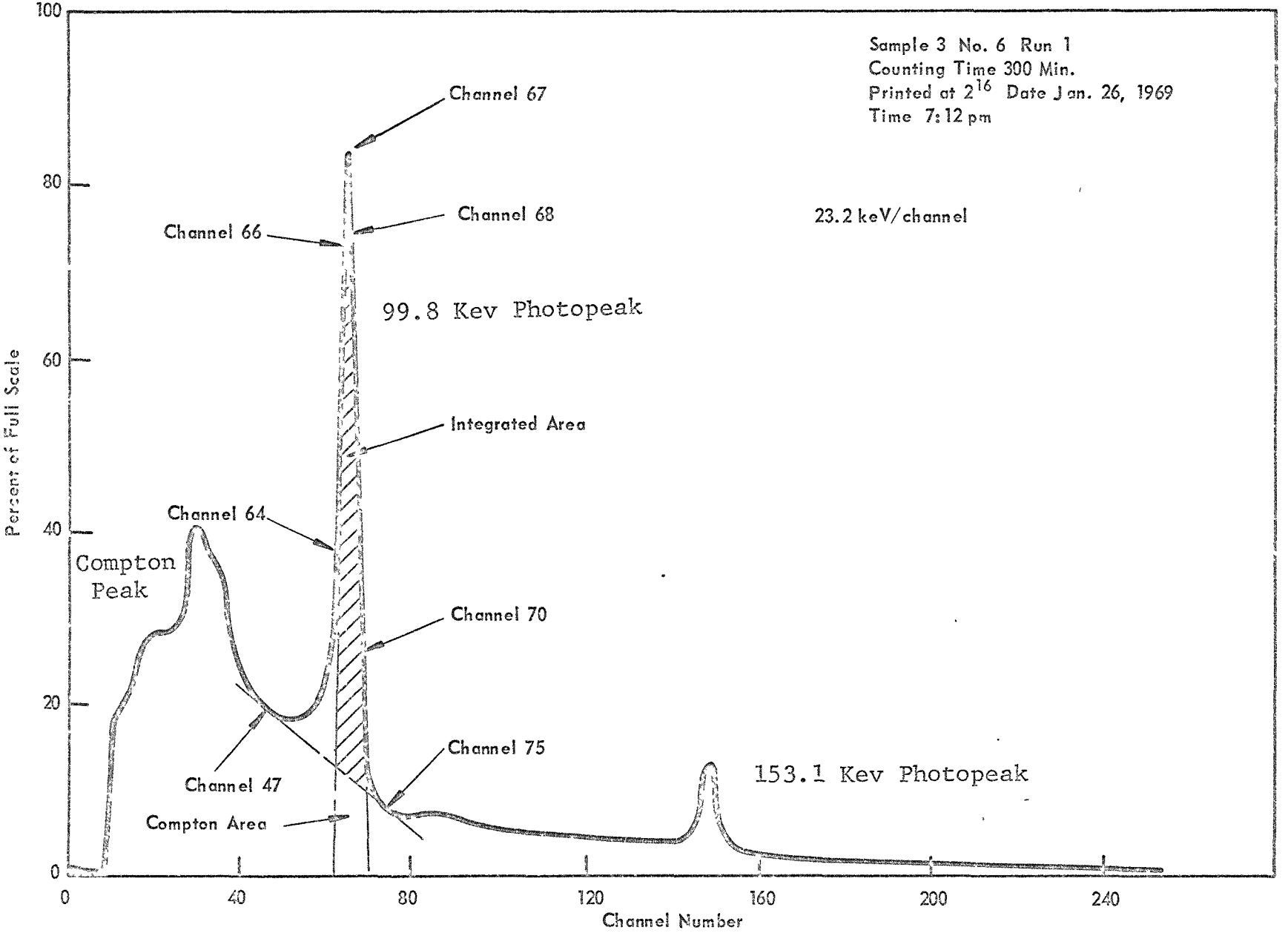

FIGURE 18: TYPICAL PLUTONIUM-238 GAMMA SPECTRUM

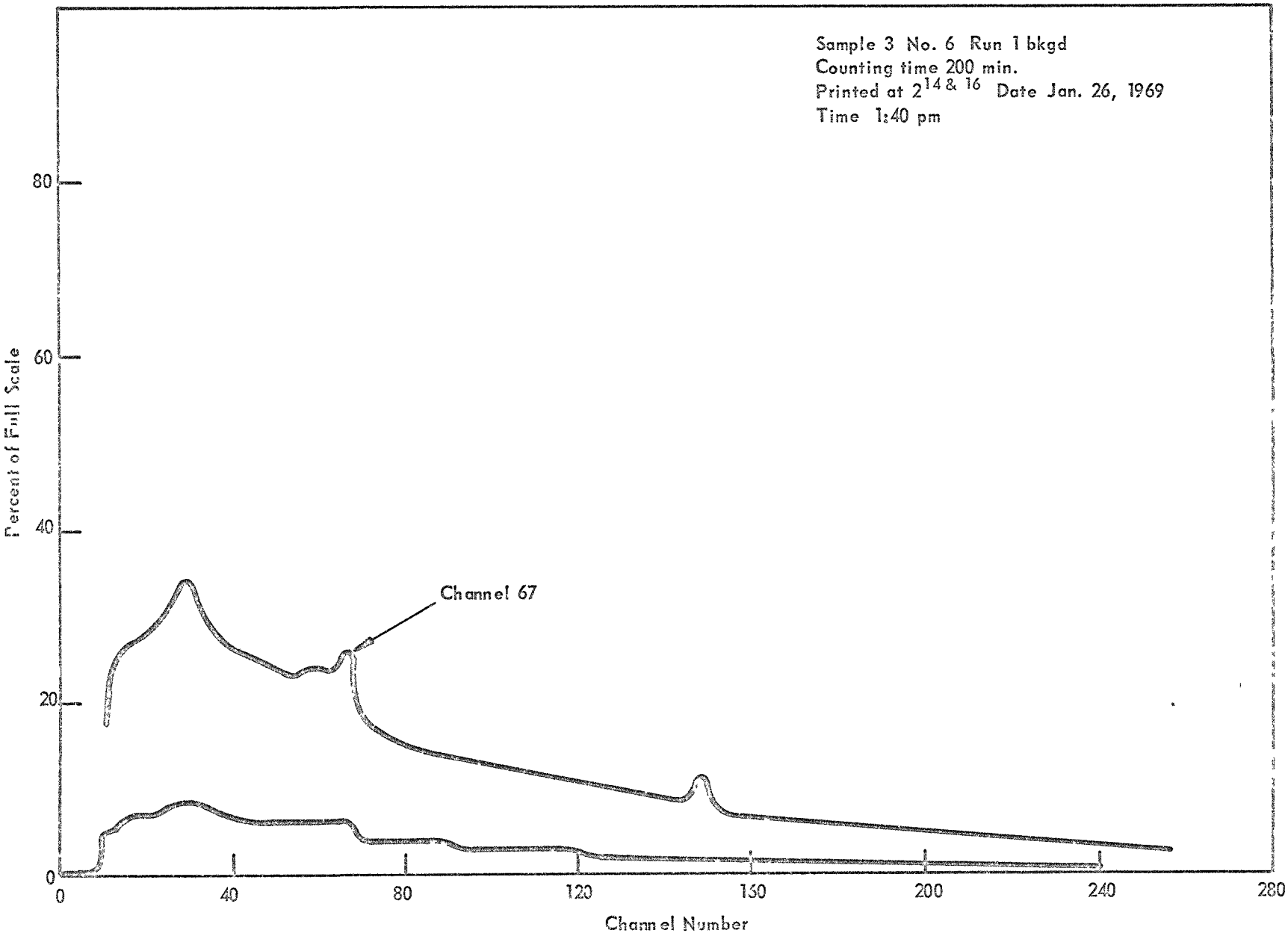

FIGURE 19: TYPICAL GAMMA BACKGROUND SPECTRUM

In three cases, the background was purposely increased so that whatever method accepted would also be independent of background fluctuations. This was a necessary restriction since the gamma counting took several weeks and the background at the laboratory varies by as much as 50 percent. The results for the precision experiment are shown in Table 6.

In analyzing the spectra, it must be understood that the gamma spectra recorded (Fig. 18) is really a charge spectra produced by the Photoelectric Effect and Compton Effect as the gamma radiation passes through the volume of the detector.[21] The Photoelectric Effect produces the full energy peaks often called "photopeaks". The Compton Effect produces a broad spectrum.

Examining the gamma spectrum (Fig. 18) again, note that the 153.1 Kev gamma peak tails off to the left and produces a Compton spectra across the entire spectrum to the left of that peak. The 99.8 Kev gamma peak sits on this Compton spectra and tails off to the left itself adding to the Compton spectra. The large broad peak at the left is the combined Compton peak from both of these gamma peaks. While we can subtract out the background, another method must be found for handling the Compton spectra on which the 99.8 Kev peak sits.

TABLE 6

GAMMA COUNTING PRECISION EXPERIMENT RESULTS

Run No.[a]	Percent Background is in Excess of Normal	Integrated Area (Total Counts)
3	25	221,313
4	100	221,526
5	100	222,012
9	0	221,466
10	0	220,963
11	0	221,227
Average and Standard Deviation		221,418±322 (±0.15%)

Theoretical Standard Deviation Based on the Square Root of the Mean Value . . . . . ±471 (±0.21%)

[a] Five pieces of data have been excluded from this table. The resolution of the detector change after Runs 1 and 2 and they did not compare (i.e., in other words, this method will not compensate for a change in resolution). The sample was not properly aligned in Run 6 and did not compare with the rest of the data. This shows the significance of careful alignment. In Runs 7 and 8, the background was increased 75 times above normal. The spectra were so distorted that the data could not be analyzed in the typical manner described and the data did not compare.

The method found most successful is shown graphically on the gamma spectrum (Fig. 18). The method consisted primarily of subtracting the background from the first and third channel on either side of the peak channel 67. These values were used to determine the slope of a line through these points and then any contributions to the triangular areas below channel 64 and beyond channel 70 could be calculated and added to the integrated total of channels 64 through 70 less the background for those channels. The integrated areas are expressed as counts. The Compton background was approximated as a straight line, the slope of which was determined by the graphical intersections of such a line. By a similar method the area below this line, expressed as counts, was calculated and subtracted from the triangular area. An example calculation is given on page 97 in Appendix B.

Using the method outlined, an integrated area expressed as total counts was obtained for each microsphere in each sample which represents the relative amount of plutonium in that microsphere. These areas are converted into ratios and percentages. The percentages represent the fraction of the total plutonium in the entire sample that each individual microsphere represents (see Tables 7, 8 and 9).

TABLE 7

THE COMPUTED GAMMA COUNTING RESULTS FOR SAMPLE 2

Microsphere Ident. No.	Integrated Area (total counts) x 10^{-5}	Relative Ratios	Percent of Total Activity
1	1.086	1.132	9.273
2	1.101	1.148	9.404
3*	1.111[a]	1.158	9.486
4	1.062	1.107	9.068
5	1.088	1.134	9.289
6*	0.959	1.000	8.191
7*	1.104	1.151	9.428
8*	1.019	1.062	8.699
9	1.107	1.154	9.453
10	0.968	1.010	8.273
11	1.105	1.152	9.436

[a] The results for microsphere Number 3 is the average of two independent runs, the results of which were 1.112×10^5 and 1.110×10^5 counts respectively.

*These microspheres were used later in the alpha counting procedure.

TABLE 8

THE COMPUTED GAMMA COUNTING RESULTS FOR SAMPLE 3

Microsphere Ident. No.	Integrated Area (total counts) $\times 10^{-6}$	Relative Ratios	Percent of Total Activity
1	1.577	1.000	10.52
2	1.949	1.236	13.00
3*	1.919	1.217	12.80
4	1.935	1.227	12.90
5	1.775	1.126	11.84
6	1.871	1.186	12.47
7*	1.938	1.229	12.92
8*	2.032	1.288	13.55

*These microspheres were used later in the alpha counting procedure.

TABLE 9

THE COMPUTED GAMMA COUNTING RESULTS FOR SAMPLE 4

Microspheres Ident. No.	Integrated Area (total counts) x 10^{-5}	Relative Ratios	Percent of Total Activity
1*	2.117	1.006	10.85
2	2.181	1.037	11.19
3	2.203	1.047	11.30
4[a]	- - - - - - - - - - -	- - - -	- - - - - - -
5	2.185	1.039	11.21
6*	2.253	1.071	11.55
7	2.170	1.032	11.13
8	2.157	1.025	11.06
9*	2.104	1.000	10.79
10*	2.129	1.012	10.92

*These microspheres were used later in the alpha counting procedure.

[a] This microsphere was lost during the gamma counting procedure.

The ratios are given to illustrate the relative amount of plutonium in each microsphere with respect to the smallest microsphere in the sample. In the gamma counting procedure it is assumed that the isotopic ratio ($^{238}Pu/^{239}Pu$) and impurities are uniform for a single sample. The stoichiometry (O/Pu) is known to be 2.000 for all three samples. Thus, ultimately, the relative gamma emission of a microsphere is indicative of the total alpha emission which is determined calorimetrically. In a study[22] run concurrently with this work, 30 samples of plutonium metal, ranging from 1 to 60,000 microwatts in thermal output, were gamma counted and calorimetered. The data from both were expressed as ratios where the smallest sample was considered to represent unity. They found excellent agreement between the two methods up to a ratio of 1.4 at which point the gamma data was consistently and increasingly lower than the calorimetry data. This was attributed to self-absorption of the gamma rays by the plutonium since calorimetry is a nearly absolute method of measurement. Of the three samples in this study, the highest single ratio was 1.288. Thus, these gamma ratios are good estimates of the total plutonium in a sample.

After all of the microspheres in a sample were gamma counted, they were placed in a microcalorimeter container and the wattage

was determined for the entire sample. This was necessary because the probable error (P.E.) could run as high as ±20% on a single microsphere. However, by calorimetering an entire sample, it is possible to reduce the P.E. to less than 0.5% for the sample. This P.E. is based on the precision of the calorimeter over hundreds of determinations and not on a number of measurements of samples 2, 3 and 4. The results reported by the Calorimetry Group at Mound Laboratory are given in Table 10.

TABLE 10

CALORIMETRY RESULTS ON SAMPLES 2, 3, AND 4

Sample No.	Microwatts (exp.)[a]	Weight of PuO_2 (μg)[b]	Alpha Emission (dis./min. $\times 10^{-9}$)[c]
2	90.0 ± 0.5	221 ± 2	5.95
3	161.0 ± 0.5	396 ± 4	10.66
4	327.5 ± 1.0	805 ± 8	21.68

[a] The error shown is the Probable Error (P.E.) as reported by the Calorimetry Group and not the Standard Deviation (σ) as used throughout this paper.

[b] These weights were calculated assuming an 80%-Pu^{238} 20%-Pu^{239} isotopic ratio and the conversion factors 1.7594 grams/watt and 88.16%-Pu in PuO_2.

[c] These values were calculated using the conversion factor 6.707×10^{7} dis./min./μ watt.[23]

V. Alpha Counting Procedure

The alpha counting was effected with a commerical Ortec model 804 vacuum counting chamber. The microsphere was placed on a stainless steel planchet (Fig. 20) which could be moved vertically or horizontally over a limited distance. An Ortec 150 square millimeter silicon surface barrier detector was used to detect the alpha radiation. The detector used had a 155 μm depletion depth which means that any alpha particle up to 16.8 Mev in energy impinging on the surface would be totally absorbed and accurately detected. It also had a gold dead layer of approximately 150Å of gold (based on 40 $\mu g/cm^2$) which is equivalent to about 20 Kev loss from a 5.5 Mev alpha particle (i.e., any alpha particle of less than 20 Kev would not penetrate the dead layer and be counted). It is considered to be 100% efficient to all energies of alpha particles as long as the total accumulated bombardment by alpha particles has not exceeded 10^9 disintegrations per square centimeter.[24],[25],[26] Since there was an aperture between the microsphere and detector, excessive damage to the detector was prohibited by occasionally realigning the planchet and aperture so that the alpha particles

DIAGRAM OF THE ALPHA COUNTING
SAMPLE ARRANGEMENT

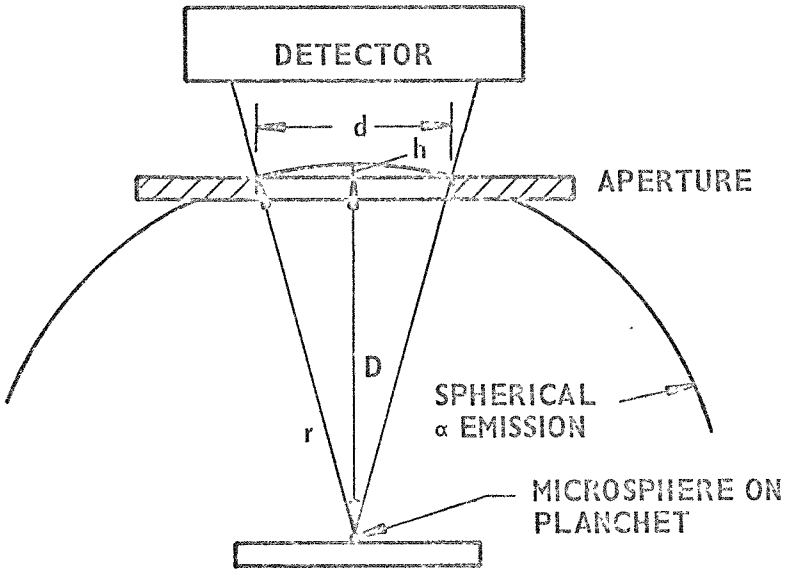

$$R = \frac{2\pi rh}{4\pi r^2} = \frac{h}{2r}$$

R = ratio of the volume of the spherical cone to the volume of the sphere.
D = distance from planchet to aperture.
d = diameter of aperture.
r = spherical radius.
h = height of zone.

$$h = r-D$$

$$r = \sqrt{D^2 + \left(\frac{d}{2}\right)^2}$$

FIGURE 20

passing through the aperture would impinge on a previously unused portion of the detector surface. Comparison of alpha counting results obtained from different areas of the detector for the same sample showed no deviation from 100% efficiency.

All alpha counting was conducted at pressures of less than 25×10^{-3} mm Hg, where the absorption of alpha particles by air is considered negligible.[26] Also, each microsphere was counted for whatever time required to attain approximately 10,000 counts in channel 239, the channel equivalent to 5.5 Mev, the maximum alpha energy from plutonium-238. The purpose for this procedure was to attain acceptable statistics in the individual channels so that the spectra could be graphically extrapolated back to the channel containing the zero energy point.

It was found that various combinations of aperture sizes and source to detector distances allowed alpha particle fluxes to reach the detector which reduced the live time of the pulse height analyzer. The pulse height analyzer has built into it a self-compensating circuit which automatically lengthens the counting time proportional to the decrease in live time. It was found that a sample count could be reproduced as long as

the live time was not allowed to drop below 90%. However, as an extra precaution to obtain the best data possible, no sample was run at less than 95% live time.

To determine the solid angle of the alpha flux being counted (refer to Fig. 20) it was necessary to make only two measurements. First, the diameter (d) of the aperture opening was measured by the Dimensional Standards Department at Mound Laboratory and the results are recorded in Table IV, Appendix A. These measurements were made in inches and then converted to centimeters for use in calculating the ratio (R). Second, it was necessary to measure the distance (D) from the surface of the planchet to the top of the aperture. In practice, identical pieces of tool steel ground flats were laid over the center of the planchet and the aperture opening and the distance (D) was measured along the center line from the planchet to the aperture with a cathatometer by sighting on the sharp edges of the ground flats. This method was found to be very precise. Any individual measurement could be easily reproduced to within ± .005 cm. Since the distance (D) recorded is the difference between two such measurements they are accurate to within ± .01 cm.

For calculating the ratio of the spherical cone of emission counted to the total spherical emission, the simple formula (derivation shown on Fig. 20)

$$R = \frac{h}{2r}$$

was not used because this would necessitate dividing a number of one significant figure (i.e., there is some uncertainty in this one figure) by a number of four significant figures (here the assumption is made that any error in the cathatometer measurements are compensating when the values are subtracted from each other).

It was found that the data could be reproduced much more precisely if the equation were expressed as:

$$R = \frac{h}{2r} = \frac{r-D}{2r} = 0.5000 - \frac{D}{2 \times \sqrt{\left(\frac{d}{2}\right)^2 + D^2}}$$

It was also found that it was necessary to keep an extra figure beyond that first significant figure in order to get good agreement between the calculated total spherical emission values.

The alpha counting results are compiled in Tables 11, 12, and 13 for Samples 2, 3, and 4, respectively. The microspheres that were alpha counted were chosen by their appearance in the 100X photomicrographs (see Figs. 14, 15, and 16). The criteria

TABLE 11

ALPHA COUNTING RESULTS FOR SAMPLE 2

Microsphere Ident. No.	Run	Counting Time (min.)	Nominal Dia. (d) (in.)	Distance (D) (cm)	Integrated Area $\times 10^{-6}$	Ratio (R) $\times 10^{4}$	Effective Activity (dis./min.) $\times 10^{-7}$
1	1	50	0.250	7.775	1.44	$4._2$	6.86
	2	50	0.350	9.290	1.96	$5._3$	6.76
	3	50	0.150	4.745	1.35	$4._0$	6.76
2	1	60	0.250	7.785	1.54	$4._2$	6.12
	2	50	0.250	6.765	1.68	$5._5$	6.10
7	1	40	0.150	3.755	1.74	$6._4$	6.80
	2	50	0.250	6.780	1.83	$5._5$	6.66
	3	40	0.250	5.760	2.02	$7._6$	6.65
8	1	60	0.150	4.745	1.52	$4._0$	6.33
	2	45	0.150	3.745	1.83	$6._4$	6.36
	3	60	0.250	7.785	1.62	$4._2$	6.43

TABLE 12

ALPHA COUNTING RESULTS FOR SAMPLE 3

Microsphere Ident. No.	Run	Counting Time (min.)	Nominal Dia. (d) (in.)	Distance (D) (cm)	Integrated Area $\times 10^{-6}$	Ratio (R) $\times 10^{4}$	Effective Activity (dis./min.) $\times 10^{-8}$
3	1	50	0.200	7.775	1.66	2.7	1.23
	2	80	0.200	9.285	1.86	1.9	1.22
	3	50	0.250	9.310	1.76	2.9	1.21
7	1	50	0.250	9.310	1.80	2.9	1.24
	2	35	0.250	7.705	1.84	4.3	1.22
	3	80	0.150	7.770	1.48	1.5	1.23
8	1	50	0.200	7.795	1.65	2.7	1.22
	2	70	0.200	9.280	1.66	1.9	1.25
	3	100	0.100	5.285	1.53	1.3	1.28

TABLE 13

ALPHA COUNTING RESULTS FOR SAMPLE 4

Microsphere Ident. No.	Run	Counting Time (min.)	Nominal Dia. (d) (in.)	Distance (D) (cm)	Integrated Area $\times 10^{-6}$	Ratio (R) $\times 10^{4}$	Effective Activity (dis./min.) $\times 10^{-8}$
1	1	80	0.150	9.310	1.46	1.0	1.82
	2	200	0.100	9.340	1.62	0.4$_5$	1.76
	3	50	0.200	9.310	1.64	1.0	1.73
6	1	100	0.100	8.165	1.12	0.6$_1$	1.84
	2	20	0.250	8.170	1.40	3.0	1.84
	3	30	0.200	8.150	1.35	2.5	1.80
	4	50	0.150	8.140	1.25	1.4	1.79
	5	20	0.100	3.190	1.45	4.0	1.81
	6	200	0.100	9.675	1.64	0.4$_3$	1.90
9	1	40	0.200	7.810	1.88	2.7	1.74
	2	40	0.200	7.805	1.86	2.7	1.72
	3	40	0.200	7.795	1.86	2.7	1.72
10	1	150	0.100	8.070	1.61	0.6$_2$	1.73
	2	40	0.200	8.035	1.72	2.5	1.72
	3	50	0.200	9.315	1.64	1.9	1.73
	4	80	0.150	9.310	1.49	1.0	1.86

for selection was a minimum of deformities and foreign matter adhering to the surfaces.

The alpha spectra shown (Fig. 21) is representative of all of the spectra obtained. It is to be noted that there is an obvious discontinuity in the low energy channels due to noise. It, therefore, had to be determined how far up the energy scale this noise extended because it was considered unlikely, but possible that the upward trend at low energies could be an indication of a large flux of low energy alpha particles. To resolve this problem, a simple experiment was performed in which the spectra was first obtained under normal conditions and then under conditions where one piece followed by a second piece of Mylar were placed over the aperture and two more spectra obtained and plotted on the same graph (Fig. 22). The purpose of this experiment was to determine if the upward tail was caused by a large flux of low energy alpha particles coming from near the end of the range of an alpha particle deep within the microsphere. If this was the case, the Mylar would absorb these low energy alpha particles and the successive plots would be linear. However, if the upward curve at the low energy end of the spectrum were due to noise in the detector, the shape of the spectra would not change. The shape of the spectra did not change and it was concluded that the upward trend was the result of noise.

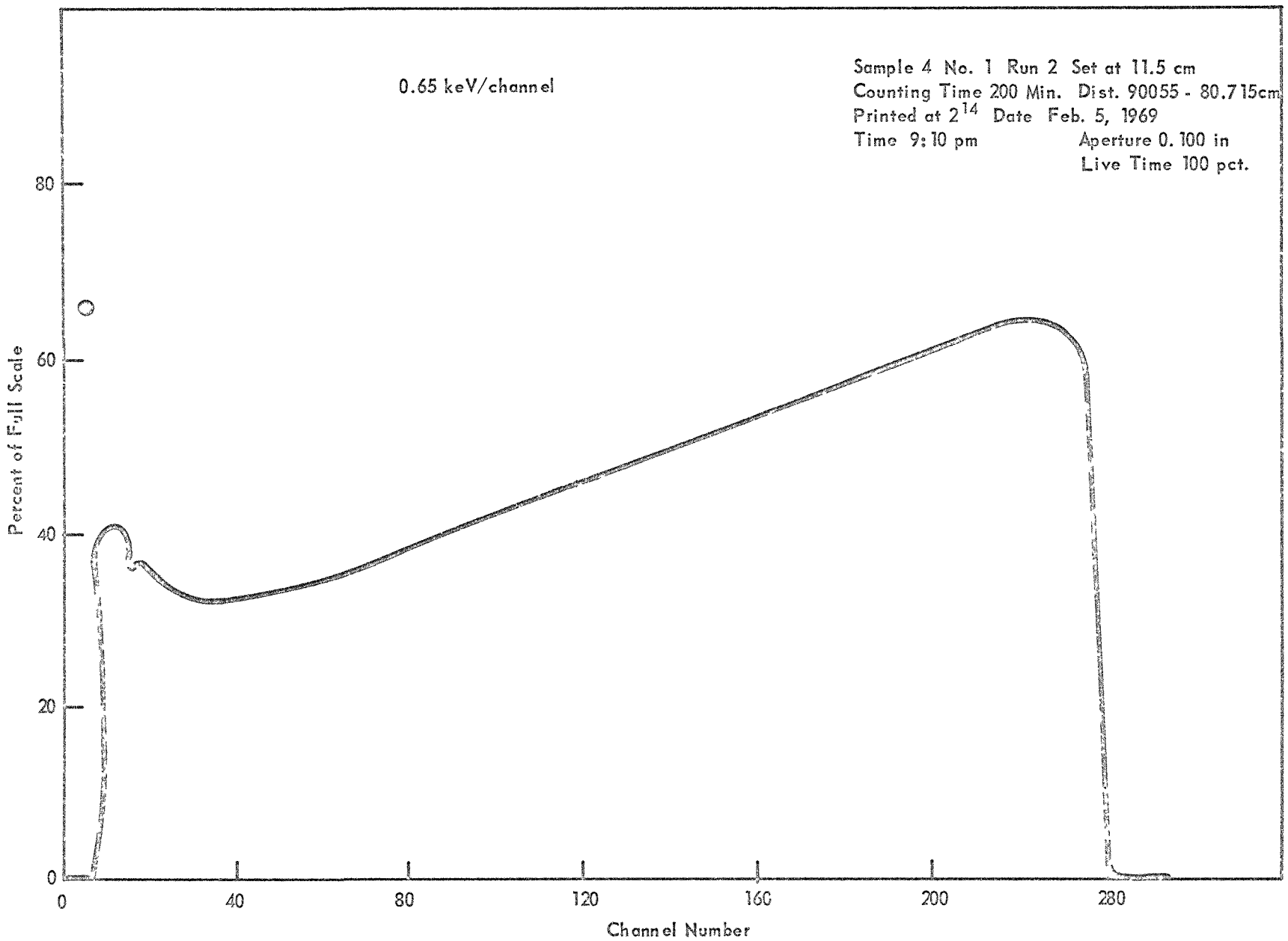

FIGURE 21: TYPICAL ALPHA SPECTRUM

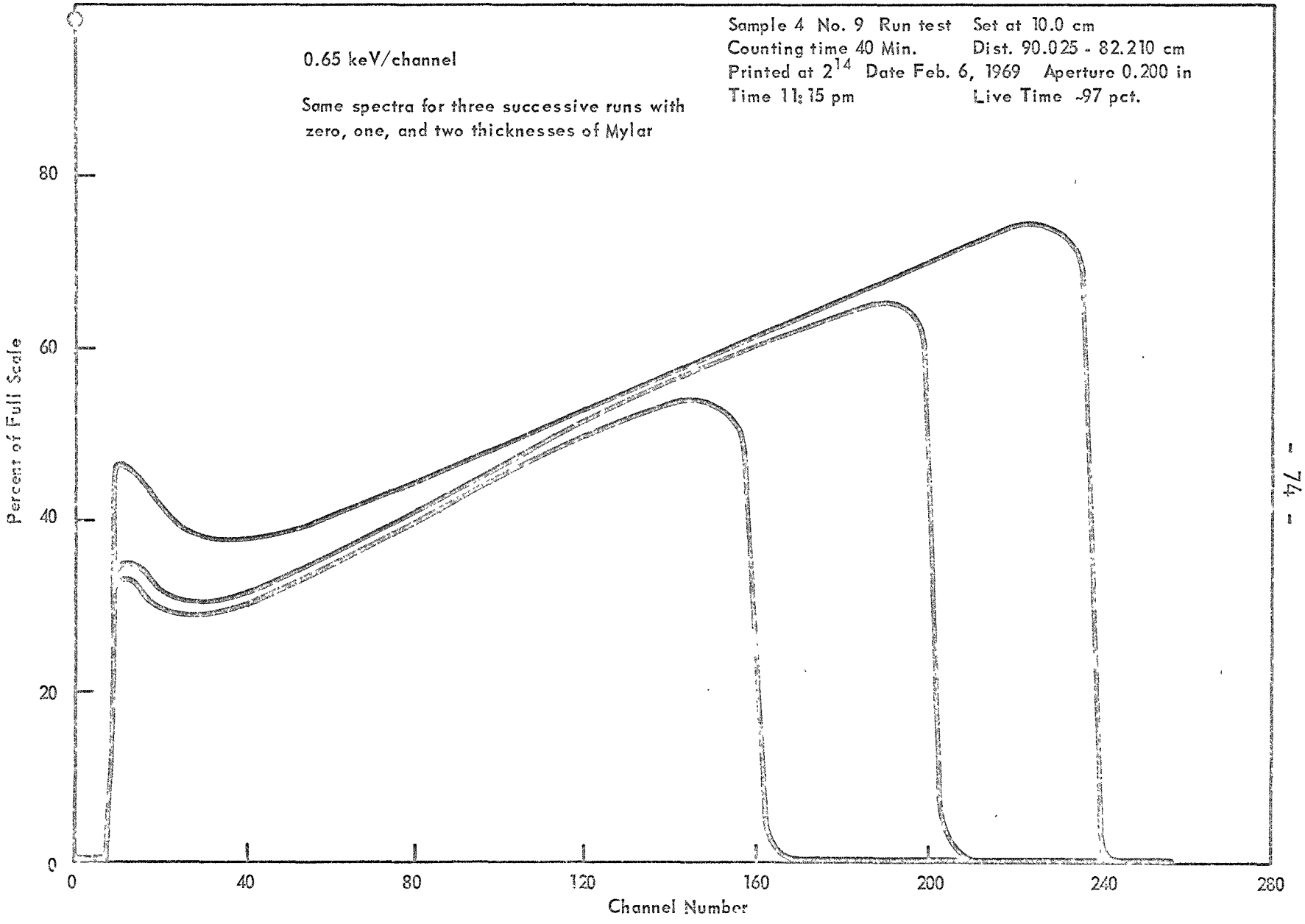

FIGURE 22: ALPHA SPECTRA FROM NOISE EXPERIMENT

An experiment was also conducted where a blank was substituted for the aperture. It was reasoned that if the upward trend were due to low energy alpha particles scattering off the sides of the counting chamber and reaching the detector without passing through the aperture, they would be counted under these conditions. In a fifty minute count only 20 counts were collected under these conditions. Therefore, alpha scattering off the walls of the chamber was discounted.

Also discounted as insignificant in this study was backscattering of alpha particles from the planchet of the counter. This is supported by studies conducted by Hutchinson, et al.[27] and calculations by Watt and Ramsden.[28] Another value discounted was background. It was checked periodically and found to be insignificantly small as compared to the total count.

Thus, the values reported as the Area Integrated in Tables 11, 12, and 13 were obtained by extrapolating the linear portion of the spectra back to the channel containing the zero energy point (i.e., channel 3) and the Integrated Area was then the total of the number of counts under this line from channel 3 to channel 79 plus the integrated total for channels 80 through channel 241 taken from the print-out tapes. An example calculation is given in Appendix B.

The zero energy point was calculated using a polonium-208 and polonium-209 standard source. Knowing the energy of the peaks and channels where they appear, one extrapolates back to zero energy. However, it can be easily seen from the alpha counting data for microsphere #9 of Sample 4 (see Table 13) that the Integrated Areas are only good to three significant figures regardless of the large total number of counts involved in the integration. This is attributed to the pulse height analyzer not being linear at the low energy end of the scale and the zero energy point is being determined by extrapolating back from the polonium peaks at the high energy end of the scale. Also, the self-compensating live time circuit in the pulse height analyzer previously discussed is not 100% accurate. Additional error of less than one percent was introduced by operating the pulse height analyzer at less than 100% live time.

RESULTS AND DISCUSSION

By experimental methods, the effective activity and diameter of several microspheres have been determined directly. However, before the equation proposed by C. J. Kershner can be satisfied so that the range of an alpha particle in PuO_2 can be calculated, the total activity of each microsphere alpha counted must be known. There are two separate methods by which we can obtain these values. The first is to assume an isotopic ratio for the microspheres and calculate the total alpha emission from the experimental weights given in Tables 2, 3, and 4. The second is to take the percentages from Tables 7, 8, and 9 and multiply these by the total alpha emissions for the entire sample given in Table 10 calculated from the calorimetry data. However, the first time this was done, the results from the two methods did not compare. The problem can best be illustrated by Table 14 which compares the experimentally determined gross sample weights with those calculated from the calorimetry results assuming an 80/20 ($^{238}Pu/^{239}Pu$) isotopic ratio and stoichiometric PuO_2. Considering the conditions under which

TABLE 14

COMPARISON OF THE EXPERIMENTAL WEIGHTS
WITH THE CALCULATED CALORIMETRIC WEIGHTS

Sample No.	Gross Sample Weight in Micrograms (exp.)[a]	Gross Sample Weight in Micrograms (calc)[b]
2	221.3	221 ± 2
3	403.2	396 ± 4
4	826.2	805 ± 8

[a] These weights can be obtained by summing the separate weights in Table 2, 3, and 4 with the exception that the weight of microsphere #4 of Sample 4 must be excluded because it was lost prior to calorimetry.

[b] These values were given previously in Table 10.

sol-gel microspheres are prepared, it is highly improbable that these microspheres would be nonstoichiometric.[10] Also, if the calculated weights were higher than those obtained experimentally, it could be explained as a thermal effect caused by the fact that the microspheres are always generating heat. The only explanation which would explain this difference in the reverse direction is that the isotopic ration ($^{238}Pu/^{239}Pu$) is not 80/20 as assumed. Therefore, the isotopic ratios were calculated approximately using the relationship?

$$\text{dis./min.} = [(x)\ (3.8147 \times 10^7\ \text{dis/min./}\mu\text{g}) + (1\text{-}x)\ (0.0137 \times 10^7\ \text{dis/min./}\mu\text{g})]\ (\mu\text{g of } PuO_2)(0.8816)$$

where x = % of Pu-238 metal

1-x = % of Pu-239 metal.

The calorimetrically determined disintegration rates from Table 10 were equated to the right hand side of this equation where the experimentally determined weight of the samples taken from Table 14 were substituted for the weight of PuO_2. The $^{238}Pu/^{239}Pu$ isotopic ratios obtained were then substituted back into a similar equation,

$$[(\%\ \text{Pu-238})\ (3.81 \times 10^7\ \text{dis/min./}\mu\text{g}) + (\%\ \text{Pu-239})\ (0.01 \times 10^7\ \text{dis/min./}\mu\text{g}) = \text{dis./min./}\mu\text{g of Pu metal}$$

The results of these calculations are compiled in Table 15. The isotopic disintegration rates used above are based on half-lives of 87.404 years for plutonium-238 and 24,145 years for plutonium-239 as determined calorimetrically by K. C. Jordan[29] of Mound Laboratory.

Using the conversion factors calculated in Table 15 and the weight data from Tables 2, 3, and 4 for those microspheres alpha counted, one can calculate the total activity of these microspheres based on their experimentally determined weights. Then, using the percentages from Tables 7, 8, and 9 for those microspheres alpha counted, and the total sample alpha emissions given in Table 10 we can obtain the total alpha emissions of these microspheres based on the calorimetric data. This data is compiled in Table 16 along with the average effective activity for each of these microspheres which were obtained by averaging the results of Tables 11, 12, and 13. Also compiled in Table 16 are the fraction (f) values which are the ratios of the effective activity to the total activity and the calculated ranges (R) of an alpha particle in PuO_2 using Kershner's relationship.

$$f = \frac{R}{16r}\left(12 - \frac{R^2}{r^2}\right) \qquad [9]$$

TABLE 15

CALCULATED CONVERSION FACTORS FOR
SAMPLES 2, 3, AND 4

Sample No.	Pu-238/Pu-239 Ratio	Weighted Conversion Factor in dis./min./μg of Pu-Metal x 10^{-7}
2	80.0/20.0	3.054
3	78.5/21.5	2.997
4	77.9/22.1	2.975

TABLE 16

THE EMISSION FRACTION (f) AND CALCULATED RANGE (R) OF AN ALPHA PARTICLE IN PLUTONIUM DIOXIDE FROM KERSHNER'S THEORY

Sample No.	Microsphere Ident. No.	Average Effective Activity (dis./min.) $\times 10^{-7}$	Weight Data			Calorimetric Data		
			Total Activity (dis./min.) $\times 10^{-8}$	Emission Fraction (f)	Range in μm (R)	Total Activity (dis./min.) $\times 10^{-8}$	Emission Fraction (f)	Range in μm (R)
2	3	6.79	5.76	0.118	12.1	5.66	0.120	12.3
	6	6.11	4.79	0.128	12.5	4.87	0.125	12.2
	7	6.70	6.70	0.120	12.3	5.60	0.120	12.3
	8	6.37	6.37	0.122	12.2	5.17	0.123	12.3
	Mean Range (μm) $\overline{R} \pm \sigma$		12.3 ± 0.1			12.3 ± 0.0$_4$		
3	3	12.2	13.8	0.0884	12.3	13.6	0.0897	12.5
	7	12.3	14.0	0.0879	12.2	13.8	0.0891	12.4
	8	12.5	14.4	0.0868	12.3	14.4	0.0868	12.3
	Mean Range (μm) $\overline{R} \pm \sigma$		12.3 ± 0.0$_5$			12.4 ± 0.1		
4	1	17.7	23.4	0.0756	12.5	23.5	0.0753	12.5
	6	18.3	25.4	0.0720	12.3	25.0	0.0732	12.5
	9	17.3	23.9	0.0724	12.0	23.4	0.0739	12.2
	10	17.6	24.1	0.0730	12.2	23.7	0.0743	12.4
	Mean Range (μm) $\overline{R} \pm \sigma$		12.2 ± 0.2			12.4 ± 0.1		
Grand Mean Range (μm) $\overline{R} \pm \sigma$			12.3 ± 0.1			12.4 ± 0.1		

In actual practice, the range (r) was estimated using Anderson's flat surface approximation,

$$f = \frac{3}{4} \frac{R}{r} \qquad [10]$$

and then 0.1 was repeatedly added or subtracted from the estimated range until a value for the fraction (f) which best satisfied the experimental data was obtained. For the diameter range in which this work was performed, the flat surface approximation never differed by more than 0.1 from the spherical value. This is not surprising since this study is in a relatively flat region of Kershner's plotted relationship (see Fig. 2), and since the radius to range ratio for these samples range from approximately 6 for the 150 μm microspheres of samples 2 to 10 for the 250 μm microspheres of sample 4.

The Bragg-Kleeman Rule[7] provides a means by which the range of an alpha particle in another medium can be used to calculate the range of an alpha particle in plutonium dioxide. Where the range of an alpha particle in air[30],[31],[32] is generally accepted as 4.1 cm at 15° C and 760 mm Hg for a 5.5 Mev alpha particle, the theoretical range of an alpha particle in plutonium dioxide of density 11.1 gm/cm^3 is 13.6 μm microns (calcuation or page 104, Appendix B). Range calculations using

the Bragg-Kleeman Rule are generally considered to be within ± 15% of the true value which covers the range of values for the experimentally determined range of an alpha particle in plutonium dioxide in this study. However, an attempt to calculate the range in plutonium dioxide from the range of a 5.5 Mev alpha particle in aluminum[83] and uranium[84] using the Bragg-Kleeman Rule gave totally unacceptable values. This was attributed to the much smaller ranges of alpha particles in these materials so that extrapolation of this type increases any error several orders of magnitude.

The most uncertain value in this study is the effective activity. The uncertainty arises in the proper interpretation of the alpha spectra. In this study, the linear portion of the alpha spectra was extrapolated to the zero energy point and all of the area under this extrapolated line was integrated. It is necessary that at zero energy there be no counts, but as just stated, the data was not treated in this manner.

It would be incorrect to force the experimental data to fit the theoretical expectation, and although the count rate must drop to zero at some energy approaching zero, the error introduced by treating the data as it was is probably very small, but nevertheless, indeterminate at this time.

Kershner's theoretical treatment of the energy spectrum (Fig. 4) gives a basis on which one could judge the error in the determination of the Integrated Area of the alpha spectrum. However, it should be remembered that the Geiger Rule on which the calculation is based is only an emperical relationship and, as such, makes the spectrum derived very questionable.

CONCLUSIONS

The range of an alpha particle in plutonium-238 dioxide is 12.3 - 12.4 microns based on Kershner's theoretical relationship:

$$f = \frac{R}{16r}\left(12 - \frac{R^2}{r^2}\right) \qquad [9]$$

This value agrees quite well with the previously estimated value of 13.6 (± 15%) microns using the Bragg-Kleeman Rule and the range of a 5.5 Mev alpha particle in air. Examination of Table 16 reveals that those samples whose mean range deviates from the grand mean have larger standard deviations which tend to overlap the value of the grand mean range. Thus, it is not unreasonable to assume that the grand mean is very close to the true range value. However, the purpose of these considerations is to show that Kershner's relationship gives highly reproducible and reasonable values and that there is no reason to believe that it does not accurately describe the relationship of the effective activity to the total activity for microspheres which have radii smaller than those investigated in this study.

Since Kershner's relationship is derived from a very general model, it is applicable to any alpha emitting microsphere. It would be interesting to study the effective activity of other alpha emitting microspheres whose alpha particles are emitted at energies considerably higher than plutonium-238. This would allow the study of Kershner's relationship over microsphere diameters in approximately the same range as used in this study, but with smaller radius to range ratios. Such an approach would yield more accurate results for the area of Kershner's relationship where the ratio of effective activity to total activity, (f), is changing rapidly (see Fig. 2). This approach would avoid the problem of the error in the radius measurement becoming more significant, because it would be proportionately greater, as the microspheres studied decreased in size.

It should be noted that Kershner's relationship provides a means by which it may be possible to accurately measure the radii of very small microspheres. It should also be considered that Kershner's relationship may be applicable to beta emitting microspheres even though they fall into the category of "light swift particles", and as such, do not have a definite range.

The results of the alpha counting do not verify a spectral model. At this time, Dr. Kershner is considering two other models besides the one reported here (Fig. 4). Any future work should attack this problem as an accurate spectral model would undoubtedly lead to new empirical relationships for the natural forces which determine the range of an alpha particle in plutonium dioxide.

BIBLIOGRAPHY

1. R. D. Evans, "The Atomic Nucleus", McGraw-Hill Book Co., New York, 1955, pp. 567-8.

2. C. F. Williamson, et al., "Tables of Range and Stopping Power of Chemical Elements for Charged Particles of Energy 0.5 to 500 Mev", CEA-R 3042, p. 4 (1966).

3. B. G. Harvey, "Nuclear Chemistry", Prentice-Hall, Inc., Englewood Cliffs, 1965, p. 72.

4. S. Glasstone, "Sourcebook on Atomic Energy", D. Van Nostrand Co., Inc., New York, 1958, pp 165-8.

5. G. Friedlander and J. W. Kennedy, "Introduction to Radiochemistry", John Wiley and Sons, Inc., New York, 1949, pp. 153-5.

6. Ibid, p. 150

7. R. D. Evans, "The Atomic Nucleus", McGraw-Hill Book Co., New York, 1955, p. 652.

8. C. J. Korshner, private communication, Monsanto Research Corporation, Miamisburg, Ohio.

9. M. E. Anderson, private communication, Monsanto Research Corporation, Miamisburg, Ohio.

10. D. L. Plymale and W. H. Smith, "The Preparation of Plutonium-238 Dioxide Microspheres by the Sol-Gel Process", MLM-1450 (April 30, 1968).

11. P. A. Hass, et al., "Sol-Gel Process Development and Microsphere Preparation", ORNL-P-2159 (1966).

12. R. G. Wymer, "Laboratory and Engineering Studies of Sol-Gel Processes at Oak Ridge National Laboratory", presented at the Panel on Sol-Gel Processes held by the International Atomic Energy Agency, Vienna, Austra, May 6-10, 1968.

13. S. G. Abrahamson, et al., "Plutonium-238 Isotopic Fuel Form Data Sheets", MLM-1564, p. 36 (Oct. 31, 1968).

14. L. V. Jones, et al., Ind. & Eng. Chem. Process Design & Development, 3, 78 (June 1964).

15. W. H. Smith, private communication, Monsanto Research Corporation, Miamisburg, Ohio

16. H. M. El-Badry, "Micromanipulators and Micromanipulation", Academic Press, Inc., New York, 1963.

17. S. W. Trefzger, private communication, Monsanto Research Corporation, Miamisburg, Ohio.

18. C. P. Shillaber, "Photomicrography: In Theory and Practice", John Wiley and Sons, Inc., New York, 1944.

19. S. G. Abrahamson, et al., "Plutonium-238 Isotopic Fuel Form Data Sheets", MLM-1564, p. 6 (October 31, 1968).

20. R. T. Overman and H. M. Clark, "Radioisotope Techniques", McGraw-Hill Book Co., Inc., New York, 1960, p. 114.

21. Available from Princeton Gamma-Tech, Inc., "Guide to the Use of Ge(Li) Detectors", Box 641, Princeton, New Jersey.

22. K. C. Jordan, private communication, Monsanto Research Corporation, Miamisburg, Ohio.

23. Unpublished data, Monsanto Research Corporation, Miamisburg, Ohio.

24. H. C. Britt and G. C. Benson, Rev. Sci. Instr., 35, 842 (1964).

25. V. A. Blinov, et al., At. Energ. (USSR), 13, 476 (Nov. 1962).

26. J. Roman, et al., "Counting-Rates, Reproducibility and Accuracy in Measuring Alpha Activity with Si(Au) Surface-Barrier Detectors", Report No. CLOR/IBJ-11-33, Institute of Nuclear Research, Central Laboratory for Radiological Protection, Warsaw, Poland (1964).

27. J. M. R. Hutchinson, et al., Intern. J. Appl. Radiation and Isotopes, 19, 517-22 (June 1968).

28. D. E. Watt and D. Ramsden, "High Sensitivity Counting Techniques", MacMillan Co., New York, 1964, pp. 109-10.

29. K. C. Jordan, "AEC Research and Development Report", MLM-1443, pp. 11-30 (March 29, 1968).

30. M. G. Holloway and M. S. Livingston, Phys. Rev., 54, 18 (1938).

31. W. P. Jesse and J. Sadauskis, Phys. Rev., 78, 1 (1950).

32. E. Rotondi and K. W. Geiger, Nucl. Instr. Methods, 40, 192-6 (1966).

33. L. C. Northcliffe, Phys. Rev., 120, 1744-57 (1960).

34. C. F. Williamson, et al., "Tables of Range and Stopping Power of Chemical Elements for Charged Particles of Energy 0.5 to 500 Mev", CEA-R3042, p. 369 (1966).

35. I. Chudacek, Czech. J. Phys., 8, 396 (1958).

APPENDIX A

The tables in Appendix A are reproductions of the Dimensional Standards Department's reports on measurements made by them in connection with this study. All measurements made by this department are made in inches. Therefore, it was necessary to convert these measurements into convenient metric units for use in the calculations of this study. Where it was important, the converted measurements have been reported in the text. However, these tables have been included to show the original data on which the calculations using these measurements are based.

TABLE I

DIMENSIONAL STANDARDS REPORT ON SAMPLE 2

Microsphere Ident. No.	Diameters at 120° Angles in Inches			Ave. Diameter and Std. Dev. in Inches[a]
	Dia. A	Dia. B	Dia. C	
1	0.6148	0.6149	0.6132	0.6143 ± 0.0007
2	0.6180	0.6153	0.6180	0.6171 ± 0.0013
3	0.6198	0.6166	0.6206	0.6190 ± 0.0017
4	0.6203	0.6168	0.6178	0.6183 ± 0.0015
5	0.6083	C.6083	0.6090	0.6085 ± 0.0003
6	0.5857	0.5851	0.5833	0.5847 ± 0.0010
7	0.6139	0.6137	0.6158	0.6145 ± 0.0009
8	0.6004	0.5991	0.5988	0.5994 ± 0.0007
9	0.6153	0.6131	0.6126	0.6137 ± 0.0012
10	0.5893	0.5899	0.5901	0.5898 ± 0.0003
11	0.6122	0.6106	0.6134	0.6121 ± 0.0011

[a] To convert these average diameters from inches to microns, multiply by 200 and divide by 0.8026.

NOTE: A stage micrometer was photographed prior to photographing the first microsphere and rephotographed after the last microsphere was photographed. It was found that 200 microns measured 0.8026 inches in both cases.

TABLE II

DIMENSIONAL STANDARDS REPORT ON SAMPLE 3

Microsphere Ident. No.	Diameters at 120° Angles in Inches			Average Diameter and Std. Dev. in Inches[a]
	Dia. A	Dia. B	Dia. C	
1	0.7781	0.7760	0.7785	0.7775 ± 0.0010
2	0.8375	0.8370	0.8383	0.8376 ± 0.0005
3	0.8351	0.8355	0.8349	0.8352 ± 0.0002
4	0.8421	0.8406	0.8437	0.8421 ± 0.0013
5	0.8046	0.8055	0.8085	0.8062 ± 0.0017
6	0.8247	0.8232	0.8250	0.8243 ± 0.0008
7	0.8366	0.8360	0.8364	0.8363 ± 0.0002
8	0.8468	0.8479	0.8482	0.8476 ± 0.0006

[a] To convert these average diameters from inches to microns, multiply by 200 and divide by 0.8026.

TABLE III

DIMENSIONAL STANDARDS REPORT ON SAMPLE 4

Microsphere Ident. No.	Diameters at 120° Angles in Inches			Average Diameter and Std. Dev. in Inches[a]
	Dia. A	Dia. B	Dia. C	
1	0.9959	0.9954	0.9980	0.9964 ± 0.0011
2	0.9990	1.0034	0.9983	1.002 ± 0.0023
3	1.0111	1.0176	1.0125	1.0137 ± 0.0028
4	1.0158	1.0221	1.0151	1.0177 ± 0.0031
5	1.0058	1.0050	1.0076	1.0061 ± 0.0011
6	1.0275	1.0268	1.0309	1.0284 ± 0.0018
7	1.0091	1.0095	1.0095	1.0094 ± 0.0002
8	1.0082	1.0061	1.0045	1.0063 ± 0.0015
9	0.9926	0.9987	0.9963	0.9959 ± 0.0025
10	1.0041	1.0087	1.0065	1.0064 ± 0.0019

[a] To convert these average diameters from inches to microns, multiply by 200 and divide by 0.8026.

TABLE IV

DIMENSIONAL STANDARDS REPORT ON THE APERTURE DIAMETERS

Nominal Dia. (in inches)	Average Diameter[a] ± % Dev.	Average Diameter (in centimeters)
0.100	0.100035 ± 0.18	0.2541
0.150	0.149450 ± 0.07	0.3796
0.200	0.201240 ± 0.02	0.5111
0.250	0.250640 ± 0.04	0.6366
0.350	0.351075 ± 0.04	0.8917
0.400	0.405950 ± 0.11	1.0311
0.450	0.451140 ± 0.01	1.1459
0.500	0.503520 ± 0.04	1.2789

[a] The Dimensional Standards Department actually only measured the high and low diameter of the aperture to the nearest millionth of an inch. The "Average Diameter" recorded is the median between these two values and the percent deviation reflects the distance from this median value to the actual high and low values measured. However, since only the first three significant figures are of any value in the calculation of the ratio (R) and the deviations in no case are large enough to effect the third significant figure, they have not been carried over in the calculation of the diameter (d) in centimeters.

APPENDIX B

THE INTEGRATED AREA FOR THE 99.8 Kev GAMMA PEAK

To determine the Integrated Area (I.A.) for microsphere number 6 of sample 3 (Fig. 18), a triangle was determined graphically and the area of the triangle, in counts, determined mathematically. Since the left side of the triangle described by channels 64, 65, and 66 is very linear and the right side of the triangle described by channels 68, 69, and 70 are also linear, lines were drawn through these points. This technique has encompassed completely, all of the counts in channels 64 through 70, thus we are able to determine the area under this portion of the peak from the printed integration tape of the pulse height analyzer. The results for the sample (S) and background (B) respectively:

S		B	
Channels	Counts	Channels	Counts
70	274,688	70	39,551
63	-37,278	63	-14,906
64-70	237,410	64-70	24,645

Since the sample was counted for 300 minutes and the background for only 200 minutes, the background must be multiplied by 1.5. Thus, the Integrated Area for channels 67-70 is:

24,645	237,410 (S)
x1.5	-36,968 (B)
36,967.5 (B)	200,442 (I.A. for 64-70)

To determine if any of the channels on either side of this group (ch. 64-70) contributes to the triangular Integrated Area, the slopes of the lines forming the sides of the triangle were calculated using the first and third channels on either side of the peak channel (i.e., ch. 67) less their respective backgrounds, using the relationship:

$$m = \frac{y-y_1}{x-x_1}$$

Since only channel 63 contributed some counts to the Area Integrated, it is the only one which will be calculated here.

$$m = \frac{(S_{66}-1.5B_{66}) - (S_{64}-1.5B_{64})}{66 - 64}$$

For channels 64 and 66 respectively,

$$m = \frac{(43,866 - 1.5 \times 3,920)-(22,883 - 1.5 \times 3,446)}{66 - 64}$$

$$m = 10,136$$

Once the slope is known, x and y can be substituted back into the above expression to obtain an expression of the type,

$$y = mx+b$$

where m is known, and b is calculated. Thus we get the equation which permits the calculation of the number of counts in channel 63:

$$y = (10,136)\ x\ -630,990$$

and where $x = 63$, then

$$y = 7,578 \text{ counts}$$

The same technique was used to calculate the contribution from channels 62, 71, and 72, but no positive values were obtained.

The base of the triangle was also determined graphically and was found to intersect channels 47 and 76 respectively. However, rather than use the number of counts found in channels 47 and 76 to calculate the slope of the line, it was found that averaging over five channels gave the best value. Thus, the average number of counts in channels 47 and 76 was taken as the average of the total number of counts found in channels 45 through 49 and 74 through 78 respectively. The values shown

below are less their respective backgrounds.

Channel	No. Cts. (S-B)	Channel	No. Cts. (S-B)
49	5,692	78	836
48	5,985	77	980
47	6,057	76	882
46	5,944	75	939
45	6,284	74	1218
Ave. for Ch. 47	5,992 counts	Ave. for Ch. 75	971 counts

Using these average values, we can now calculate the slope:

$$m_2 = \frac{971 - 5,992}{76 - 47}$$

$$m_2 = -173,137$$

Rearranging the above expression,

$$y = (-173,137)x + 14,129$$

we are now able to calculate the number of counts under the base line of the triangle which must be subtracted from the Integrated Area calculated above. Since their are 8 channels from channel 63 to channel 70, the number of counts at the midpoint is calculated and multiplied by 8, i.e.,

	ch. 66.5	2616 counts
		x8
Ch. 63-70	(Compton Background)	20,927 counts

Combining the three values calculated, we get the Integrated Area reported:

$$200,442 + 7,578 - 20,927 = 187,093 \text{ I.A.}$$

THE INTEGRATED AREA FOR THE ALPHA SPECTRA

Graphically, all of the alpha spectra appeared to be linear between channels 60 and 220. However, when mathematically determining the slope, an average of 41 channels was taken. Using the total counts from the integration tape printed by the pulse height analyzer for channels 200, 159, 120, and 79 as shown below for microsphere number 1 of sample 4 (Fig. 21) one obtains the total number of counts in 41 channels:

Ch. 200	1,283,262	Ch. 120	639,436
Ch. 159	- 930,542	Ch. 79	-379,851
ch. 160-200	352,720 counts	ch. 80-120	259,585 counts

Since the midpoint between channels 160 and 200 is channel 180, and the midpoint between channels 80 and 120 is channel 100: 352,720 ÷ 41 = 8,603 Ave. counts in Ch. 180

259,585 ÷ 41 = 6,331 Ave. counts in Ch. 100

The slope of the graphically determined line can now be calculated by using the expression:

$$m = \frac{y-y_1}{x-x_1}$$

Substituting the average number of counts in channels 180 and 100 respectively:

$$m = \frac{8603 - 6331}{180 - 100}$$

$$m = 28,400$$

Substituting x and y back into the above expression, we can now rearrange this result to get the more useful expression:

$$y = (28,400)\, x + 3491$$

Since the zero energy point lies in channel 3 and channel 79 is the last channel to be mathematically integrated, we calculate the number of counts in the midpoint channel (i.e., ch. 41) and multiply that value by the total number of channels (i.e., 77)

ch. 41	4655
	x77
Ch. 3-79	358,466

From the integration tape we can obtain the total number of counts beneath the alpha spectra from channel 80 through channel 241:

ch. 80	1,641,917	
ch. 241	- 379,851	
Ch. 80-241	1,262,066	counts

The Integrated Area (I.A.) is the sum of that portion from the tape and that portion mathematically integrated

ch. 3-79	358,466	
ch. 80-241	1,262,066	
	1,620,532	I.A. reported

THE THEORETICAL RANGE USING THE BRAGG-KLEEMAN RULE

Using the reduced form of the Bragg-Kleeman Rule,

$$R_{PuO_2} = 3.21 \times 10^{-4} \frac{\sqrt{A}_{PuO_2} R_{air}}{\rho_{PuO_2}}$$

where thr range of an alpha particle in air, R_{air}, is taken to be 4.1 cm, thc density, ρ_{PuO_2}, of the plutonium dioxide microsphere is 11.1 gm cm^{-3}, and the effective atomic weight is calculated as

$$\sqrt{A}_{PuO_2} = \frac{(1/3)(238.2) + (2/3)(16)}{(1/3)\sqrt{238.2} + (2/3)\sqrt{16}}$$

$$\sqrt{A}_{PuO_2} = 11.5 \ (gm)^{\frac{1}{2}}$$

we can obtain the range of an alpha particle in plutonium dioxide R_{PuO_2}. The value for the atomic weight of plutonium was arrived at by assuming an 80/20 ($^{238}Pu/^{239}Pu$) isotopic ratio, i.e.

$$(0.8)(238) + (0.2)(239) = 238.2 \text{ gm}$$

Making all of the proper substitutions, the range of an alpha particle in plutonium dioxide is

$$R_{PuO_2} = 13.6 \ \mu m.$$